ACS OMEGA

http://pubs.acs.org/journal/acsodf

Article

Peptidomics of *Haemonchus contortus*

Armelle Buzy,* Camille Allain, John Harrington, Dominique Lesuisse, Vincent Mikol, David F. Bruhn, Aaron G. Maule, and Jean-Claude Guillemot

Cite This: *ACS Omega* 2021, 6, 10288−10305

Read Online

ACCESS | Metrics & More | Article Recommendations | Supporting Information

ABSTRACT: The nematode *Haemonchus contortus* (the barber's pole worm) is an endoparasite infecting wild and domesticated ruminants worldwide. Widespread anthelmintic resistance of *H. contortus* requires alternative strategies to control this parasite. Neuropeptide signaling represents a promising target for anthelmintic drugs. Identification and relative quantification of nematode neuropeptides are, therefore, required for the development of such therapeutic targets. In this work, we undertook the profiling of the whole *H. contortus* larvae at different stages for the direct sequencing of the neuropeptides expressed at low levels in these tissues. We set out a peptide extraction protocol and a peptidomic workflow to biochemically characterize bioactive peptides from both first-stage (L1) and third-stage larvae (L3) of *H. contortus*. This work led to the identification and quantification at the peptidomic level of more than 180 mature neuropeptides, including amidated and nonamidated peptides, arising from 55 precursors of *H. contortus*. The differential peptidomic approach provided evidence that both life stages express most FMRFamide-like peptides (FLPs) and neuropeptide-like proteins (NLPs). The *H. contortus* peptidome resource, established in this work, could add the discovery of neuropeptide system-targeting drugs for ruminants.

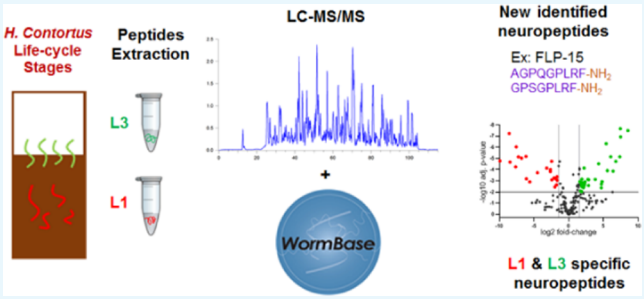

INTRODUCTION

Haemonchus contortus is a very common endoparasite and one of the most pathogenic nematodes infecting wild and domesticated ruminants worldwide.[1] It lives in the abomasum, causing hemorrhagic gastritis, anemia, edema, and even death of the infected animals.[2]

H. contortus exhibits a monoxenous life cycle that consists of a free-living phase in the external environment and a parasitic phase in the infested host animal.[3] The life cycle begins with the laying of eggs by *H. contortus* females. The first-stage larvae (L1s) develops inside the eggs after their excretion in the host feces and molts to the second stage (L2s) and then into the third-stage larvae (L3s) within approximately 1 week. The infective L3s are then ingested by the host animal, undergo an exsheathment process to develop to become fourth-stage larvae (L4s) and then to dioecious adults within 3 weeks in the stomach. The last two stages feed on blood from capillaries of the abomasal wall.

Haemonchosis is mainly controlled by anthelmintics, which act by compromising the nematode motor function.[4−6] However, the increase in resistance to existing chemotherapeutics warrants the identification of new parasiticides with novel modes of action.[7−9] As neuropeptides and their receptors regulate many vital biological processes (such as development, behavior, movement, metabolism, and reproduction[5,10]), the nematode neuropeptide signaling system has been proposed as a promising target for novel drugs against helminths.[11] Neuropeptides consist of short peptides that are derived from larger precursor proteins by the action of processing enzymes and are commonly subjected to post-translational modifications.[12] Three large neuropeptide groupings occur in nematodes, two of which are defined by conserved structural features (the FMRFamide-like peptides (FLPs)[12−15] and insulin-like peptides (INSs)).[16] The FMRFamide-like peptides (FLPs) are a group of neuropeptides that are similar to the tetrapeptide FMRF-amide (H-Phe-Met-Arg-Phe-NH2), a cardioexcitatory peptide first isolated from the mollusk *Macrocallista nimbosa*.[17] Neuropeptides sharing a C-terminal RFamide motif have been further identified from other organisms and were defined as FLPs. The third group comprises all other neuropeptides and includes diverse family groupings (the neuropeptide-like proteins NLPs.) Unlike FLPs and INSs that each comprise single families, the NLPs were originally defined as encompassing 11 distinct peptide families.[18,19] The most studied neuropeptide family in nematodes is the FLP gene family: all contain a variation in the tetrapeptide motif X/Y-X-

Received: February 4, 2021
Accepted: March 29, 2021
Published: April 7, 2021

https://doi.org/10.1021/acsomega.1c00650
ACS Omega 2021, 6, 10288−10305

Table 1. Presence of FMRFamide-like Peptide Encoding Genes (FLPs) in Genomic and Transcriptomic Data Sets of *H. contortus*

flp-gene	Presence of a flp gene sequologue[a]	C-terminal FLP motif[a]	*H. contortus* Sequelogues[a]	Presence in PRJEB506	Presence in PRJNA205202
flp-1	yes:	PNFLRFG	KPNFMRFG	yes	yes
	7 predicted peptides		GSDPNFLRFG	yes	yes
			NQPNFLRFG (2×)	yes	yes
			AAGDPNFLRFG	yes	yes
			GAGDPNFLRFG	yes	yes
			GVDPNFLRFG	yes	yes
			KPNFLRFG	yes	yes
flp-2	yes:	REPXoRFG	FRGEPIRFG	yes	no
	2 predicted peptides		VPREPIRFG	yes	no
flp-3	no	LG(T/Xo)MRFG			
flp-4	no	KPTFIRFG			
flp-5	yes	(P/Q)K(F/L)IRFG	APKFIRFG	yes	yes
	2 or 3 predicted peptides		AGGAKFIRFG	yes but **G**GGAKFIRFG	yes but **G**GGAKFIRFG
			AAKFIRFG (no described for *H. contortus*)	yes: AAKFIRFG	no
flp-6	yes: 1 predicted peptide	KSAYMRFG	KSAYMRFG (5×)	yes	yes
flp-7	yes: 4 predicted peptides	PXoXiRSXXoXoRFG	SSIFRFG	yes but TPMVRSSMVRFG	no
			APMDRSAMVRFG (2×)	yes	no
			APMDRSSMVRFG (2×)	yes	no
flp-8	yes: 1 predicted peptide	KNEFXoRFG	KNEFIRFG	yes	no
flp-9	yes: 1 predicted peptide	KPSFVRFG	KPSFVRFG (2×)	yes	no
flp-10	no	YXoRFG			
flp-11	yes: 3 predicted peptides	RNXLXoRFG	AMRNALVRFG	yes	no
			AGGSMRNALVRFG	yes	no
			YLATDDDYATAAAQG	yes	no
			NGAPQPFVRFG	yes	no
flp-12	yes: 1 predicted peptide	NKFEFIRFG	NKFEFIRFG	yes	no
flp-13	yes: 7 predicted peptides	PLXoRFG	SFEENASPLIRFG	yes	no
			DLSGAPLIRFG	yes	no
			APEAHPLIRFG	yes	no
			APDSAPLIRFG	yes	no
			DPEASPLIRFG	yes	no
			SPAAPLIRFG	yes	no
			SPNASPLIRFG	yes	no
flp-14	yes: 2 predicted peptides	KHEYLRFG	KHEYLRFG (4×)	yes	yes
			KHEYLRFSRFG	no	no
flp-15	yes: 2 predicted peptides	PXGPLRFG	AGPQGPLRFG	yes	yes
			RGPSGPLRFG	yes	yes
flp-16	yes: 2 predicted peptides	(A/G)QTFVRFG	AQTFVRFG (2×)	yes	no
			GQTFVRFG (2×)	no	no
flp-17	yes: 2 predicted peptides	KSAFVRFG	KSAFVRFG	yes	yes
			KSQYIRFG	yes	yes
flp-18	yes: 8 predicted peptides	PGXoXoRFG	XLVGGMPGVLRFG	yes but DLDGGMPGVLRFG	yes but DLDGGMPGVLRFG
			EVPGVLRFG	yes	yes
			CMPGVLRFG	yes but SMPGVLRFG	yes but SMPGVLRFG
			SVPGVLRFG	yes	yes
			EMPGVLRFG	yes	yes
			AMPGVLRFG	ys	yes
			TEIPGLMRFG	yes but TEIPGMMRFG	yes but TEIPGMMRFG
			NVPGVLRFG	yes	yes
flp-19[b]	yes: 2 predicted peptides	WXXQXoRFG	WANQVRFG	yes (WBPS10)	no
			ASSWASSIRFG	yes (WBPS10)	no
flp-20	yes: 2 predicted peptides	AXoXoR(L/F)G	AMMRLG	no	no
			AIMRLG	no	no
flp-21	yes: 1 predicted peptide	GPRPLRFG	GLGPRPLRFG	yes	yes
flp-22	yes: 3 predicted peptides	KWMRFG	TPSAKWMRFG	yes	no
			SPNAKWMRFG	yes	no
			TPDAKWMRFG	yes	no
flp-23	yes: 1 predicted peptide	Q(D/N)FLRFG	LQDFLRFG	no	no
flp-24	yes: 1 predicted peptide	DMMXoRFG	VPSAGDMMVRFG	yes	no
flp-25	yes: 2 predicted peptides	YD(Y/F)XoRFG	HYDFVRFG	yes	yes
	no		ASYDYIRFG	yes	yes
flp-26	*no*	DL(T/A)LRFG			
flp-27	no	GXRMRFG			
flp-28	yes	(I/V)XoMRFG	IFMRFG	no	yes
flp-31	no	RPRGPPRFG			
flp-32	yes: 1 predicted peptide	AMRN(S/A)LXoRFG	AMRNSLVRFG	no	no
flp-33	yes: 1 predicted peptide	XoXoDXXoQKPRFG	SIDEIQKPRFG	yes	yes
flp-34	yes: 2 predicted peptides	SAINSAGRLRYG	SDLSDFASAINSAGRLRYG	yes	yes
			APITSKLIQSLNEAERLRFG	yes	yes

[a]From McCoy et al.[14] gray shading indicates the presence of a gene. The number of copies of a predicted peptide is indicated as (no.×). Complete sequence of *flp-32* was found in Atkinson et al.[35] X_0 denotes a hydrophobic amino acid. One peptide among the four amidated peptides predicted from the *flp-11* precursor is not an *flp* peptide. This peptide is indicated in italics. [b]*flp-19* sequence was present in previous PRJEB506 release (versions to 10) but not in versions 11−14.

https://doi.org/10.1021/acsomega.1c00650
ACS Omega 2021, 6, 10288−10305

RF-amide where X is a nonpolar hydrophobic (L, I, M or V) residue and Y is aromatic.[12,14,15,20]

Detailed knowledge on neuropeptide sequences in parasitic nematodes and their post-translational modifications is required to help building an understanding of their *in vivo* biology and physiological role. The availability of genomic and transcriptomic data sets and the development of *in silico* mining tools have enabled the identification of neuropeptide genes and further prediction of neuropeptide sequences.[21−23] However, these *in silico* discovery approaches suffer major drawbacks in that the end products are bioactive peptides that can be modified, nonclassically cleaved, or even mispredicted.[24] The development and application of sensitive mass spectrometry-based peptidomic technologies[25] have enabled the biochemical identification of many nematode neuropeptides.[22,26,27] Of particular interest is the recent work performed on *Caenorhabditis elegans* in which a peptidomic analysis was performed to identify unprecedented 203 mature neuropeptides from *C. elegans*.[28,29] Previous high-throughput peptidomic approaches on parasitic nematodes have been confined to the large gastrointestinal parasite of pigs, *Ascaris suum*.[22,30] No such studies have been reported on other nematode parasites and only two FLP neuropeptides have been characterized biochemically from *H. contortus*.[31,32] In this paper, we report on a comprehensive peptidomic study to biochemically monitor, identify, and quantify endogenous peptides from two larval stages (the first-stage larvae (L1s) and the third-stage larvae (L3s)) of *H. contortus* through a peptidomic workflow using the recent release of two genome assemblies for *H. contortus*.[33,34]

This study aimed at characterizing the whole-worm peptidome of L1 and L3 larval stages of *H. contortus* using a label-free peptidomic approach. Peptidome exploration of essential developmental stages of *H. contortus* will provide a valuable repository for a better understanding of this nematode at the biochemical level.

RESULTS

Genomic and Transcriptomic Data Set Interrogation. The direct identification of bioactive peptides using a mass spectrometry (MS)-based strategy relies on mapping the peptide masses identified to a reference data set (predicted from genome and/or transcriptome). There are two genomic and transcriptomic data sets publicly available for *H. contortus*.[33,34] The two versions of the genome and transcriptome presented in both publications are available on the WormBase site (https://wormbase.org) (BioProject PRJNA205202 and BioProject PRJEB506). The protein FASTA files for both BioProjects can be downloaded from the WormBase site. It is noteworthy that for the BioProject PRJEB506, the genome reported for *H. contortus* has been updated in the WormBase version 11.0, whereas all of the PRJNA205202 versions have remained unchanged.

Before submitting MS/MS data for database searching, we analyzed the two *H. contortus* draft genomes and transcriptomes, PRJNA205202 version 14 (WBPS14) and PRJEB506 version 14 (WBPS14) and version 10 (WBPS10), for the presence of potential FLPs using the *H. contortus* C-terminal FLP motifs and FLP-gene sequelogues identified by McCoy et al. in a pan-phylum bioinformatics study[14] (Table 1).

Among the 32 FLP-encoding genes identified in 17 nematode parasites, 26 have been reported for *H. contortus*, highlighted in gray in Table 1.[14,36] Each *flp* gene encodes one or several FLPs, up to 8, for a total of 62 different predicted FLPs. Eleven FLP sequences (*flp-1, flp-5, flp-6, flp-14, flp-15, flp-17, flp-18, flp-21, flp-25, flp-33*, and *flp-34*) were identified within both the *H. contortus* databases reported in PRJEB506 and PRJNA205202 (WormBase), with some discrepancies in sequences for *flp-5*, *flp-14*, and *flp-18* (Table 1). Eleven *flp* transcripts (*flp-2, flp-7, flp-8, flp-9, flp-11, flp-12, flp-13, flp-16, flp-19, flp-22*, and *flp-24*) were found only in PRJEB506 with some discrepancies in sequence for *flp-7* and *flp-16*. *Flp-28* was only identified in PRJNA205202. Surprisingly, *flp-19* was present in previous PRJEB506 releases (versions 1−10) but not in versions 11−14. Finally, three *flp* sequences (*flp-20, flp-23*, and *flp-32*) were not identified in either database (Figure 2); *flp-32* was reported by Atkinson et al.[35]

To maximize peptide identification using our approaches, we used a combination of the two transcriptome databases (PRJEB506 and PRJNA205202) with a homemade database that we constructed from the sequelogue sequences described[14] (Supplementary Data 1).

Identification of Neuropeptides. To biochemically identify endogenous FLP peptides and other bioactive peptides of *H. contortus*, a peptide acidic/methanol extraction method was used (see the Methods section). Peptides extracted from both first-stage (L1) and third-stage larvae (L3) of *H. contortus* were analyzed by LC/MS/MS, and the results were processed in the MaxQuant environment implemented with the three FASTA databases described in the above paragraph. This way, we sequenced 181 endogenous peptides belonging to 55 different peptide precursor proteins.

FMRFamide-like Peptides. Among the 26 FLP genes described for *H. contortus*, there are 62 predicted FMRFamide-like peptides (Table 1). In addition, two peptides not strictly belonging to the FLPs can be found, the *flp-11* peptide (YLATDDDYATAAAQG) described as a neuropeptide and the RYamide *flp-34* peptide (SDLSDFASAINSAGRLRYG).

In this work, we isolated and identified 54 of the 62 predicted peptides (Table 2) across the two larval stages. Only two of these peptides were previously biochemically characterized, KHEYLRF.NH_2 (*flp-14*) and KSAYMRF.NH_2 (*flp-6*), by Keating et al.[31] and Marks et al.[32]

All predicted FLP precursors were found except *flp-20, flp-21, flp-23, flp-28*, and *flp-32*. It is noteworthy that *flp-20, flp-23*, and *flp-32* were not identified in either of the WormBase data sets, although the complete *flp-32* sequence was previously reported.[35] In the study performed on *C. elegans* by Van Bael et al.,[28,29] the bioactive peptides issued from these precursors were either not detected or could not be confirmed using MS/MS. Peptides predicted to be encoded by *flp-1, flp-2, flp-6, flp-8, flp-9, flp-11, flp-12, flp-13, flp-15, flp-17, flp-19, flp-24, flp-25, flp-33*, and *flp-34* transcripts, which had identical sequences between those reported in MacCoy et al.[14] and both WormBase databases, were all unambiguously identified in this study, except for one peptide (APITSKLIQSLNEAERLRFG) arising from *flp-34* (Table 1), not detected in this study. Peptides arising from *flp-19* (WANQVRFG and ASSWAS-

https://doi.org/10.1021/acsomega.1c00650
ACS Omega 2021, 6, 10288−10305

Table 2. FLP-Amidated Peptides Identified in the First-Stage (L1) and Third-Stage Larvae (L3) of *H. contortus*

gene	precursor name[a]	database	sequence	modifications	mass	start position	end position
flp-1	HCON_00103480; maker-scaffold1982-snap-gene-0.20-mRNA-1	PRJEB506; PRJNA205202	KPNFMRFG	Gly-loss +Amide	937.4956	70	77
flp-1	HCON_00103480; maker-scaffold1982-snap-gene-0.20-mRNA-1	PRJEB506; PRJNA205202	GSDPNFLRFG	Gly-loss +Amide	1050.525	87	96
flp-1	HCON_00103480; maker-scaffold1982-snap-gene-0.20-mRNA-1	PRJEB506; PRJNA205202	NQPNFLRFG	Gly-loss +Amide	1033.546	98	106
flp-1	HCON_00103480; maker-scaffold1982-snap-gene-0.20-mRNA-1	PRJEB506; PRJNA205202	AAGDPNFLRFG	Gly-loss +Amide	1105.567	118	128
flp-1	HCON_00103480; maker-scaffold1982-snap-gene-0.20-mRNA-1	PRJEB506; PRJNA205202	GAGDPNFLRFG	Gly-loss +Amide	1091.551	130	140
flp-1	HCON_00103480; maker-scaffold1982-snap-gene-0.20-mRNA-1	PRJEB506; PRJNA205202	GVDPNFLRFG	Gly-loss +Amide	1062.561	143	152
flp-1	HCON_00103480; maker-scaffold1982-snap-gene-0.20-mRNA-1	PRJEB506; PRJNA205202	KPNFLRFG	Gly-loss +Amide	919.5392	154	161
flp-2	HCON_00188000	PRJEB506	FRGEPIRFG	Gly-loss +Amide	1019.567	39	47
flp-2	HCON_00188000	PRJEB506	VPREPIRFG	Gly-loss +Amide	1011.598	50	58
flp-5	HCON_00164350; maker-scaffold856-augustus-gene-0.7-mRNA-1	PRJEB506; PRJNA205202	APKFIRFG	Gly-loss +Amide	876.5334	37	44
flp-5	HCON_00164350; maker-scaffold856-augustus-gene-0.7-mRNA-1	PRJEB506; PRJNA205202	GGGAKFIRFG	Gly-loss +Amide	950.545	46	55
flp-5	HCON_00164350; maker-scaffold856-augustus-gene-0.7-mRNA-1	PRJEB506	AAKFIRFG	Gly-loss +Amide	850.5177	80	87
flp-6	HCON_00155670; augustus-scaffold18780-abinit-gene-0.3-mRNA-1	PRJEB506; PRJNA205202	KSAYMRFG	Gly-loss +Amide	900.464	32	39
flp-7	HCON_00164220	PRJEB506	TPMVRSSMVRFG	Gly-loss +Amide	1308.68	42	53
flp-7	HCON_00164220	PRJEB506	APMDRSAMVRFG	Gly-loss +Amide	1278.633	56	67
flp-7	HCON_00164220	PRJEB506	APMDRSSMVRFG	Gly-loss +Amide	1294.627	97	108
flp-8	HCON_00180390	PRJEB506	KNEFIRFG	Gly-loss +Amide	951.529	3	10
flp-9	HCON_00131250	PRJEB506	KPSFVRFG	Gly-loss +Amide	878.5127	69	76
flp-11	HCON_00176100	PRJEB506	AMRNALVRFG	Gly-loss +Amide	1075.607	31	40
flp-11	HCON_00176100	PRJEB506	AGGSMRNALVRFG	Gly-loss +Amide	1276.682	42	54
flp-11	HCON_00176100	PRJEB506	YLATDDDYATAAAQG	Gly-loss +Amide	1486.658	57	71
flp-11	HCON_00176100	PRJEB506	NGAPQPFVRFG	Gly-loss +Amide	1130.599	74	84
flp-12	HCON_00164300	PRJEB506	NKFEFIRFG	Gly-loss +Amide	1098.597	74	82
flp-13	HCON_00095850	PRJEB506	SFEENASPLIRFG	Gly-loss +Amide	1407.715	44	56
flp-13	HCON_00095850	PRJEB506	DLSGAPLIRFG	Gly-loss +Amide	1086.619	59	69
flp-13	HCON_00095850	PRJEB506	APEAHPLIRFG	Gly-loss +Amide	1148.646	71	81
flp-13	HCON_00095850	PRJEB506	APDSAPLIRFG	Gly-loss +Amide	1084.603	84	94
flp-13	HCON_00095850	PRJEB506	DPEASPLIRFG	Gly-loss +Amide	1142.608	96	106
flp-13	HCON_00095850	PRJEB506	SPAAPLIRFG	Gly-loss +Amide	969.576	109	118
flp-13	HCON_00095850	PRJEB506	SPNASPLIRFG	Gly-loss +Amide	1099.614	120	130
flp-14	HCON_00084500; maker-scaffold19612-snap-gene-0.18-mRNA-1	PRJEB506; PRJNA205202	KHEYLRFG	Gly-loss +Amide	990.5399	93	100
flp-15	HCON_00084140	PRJEB506; PRJNA205202	AGPQGPLRFG	Gly-loss +Amide	940.5243	41	49
flp-15	HCON_00084140	PRJEB506; PRJNA205202	GPSGPLRFG	Gly-loss +Amide	828.4606	53	61
flp-16	HCON_00035475	PRJEB506	AQTFVRFG	Gly-loss +Amide	866.4763	70	77

https://doi.org/10.1021/acsomega.1c00650
ACS Omega 2021, 6, 10288−10305

Table 2. continued

gene	precursor name[a]	database	sequence	modifications	mass	start position	end position
flp-17	HCON_00123460; maker-C469629-augustus-gene-0.17-mRNA-1	PRJEB506; PRJNA205202	KSAFVRFG	Gly-loss +Amide	852.497	72	79
flp-17	HCON_00123460; maker-C469629-augustus-gene-0.17-mRNA-1	PRJEB506; PRJNA205202	KSQYIRFG	Gly-loss +Amide	939.529	112	119
flp-18	HCON_00164730; augustus-scaffold2866-abinit-gene-0.0-mRNA-1	PRJEB506; PRJNA205202	DLDGGMPGVLRFG	Gly-loss +Amide	1274.644	54	66
flp-18	HCON_00164730; augustus-scaffold2866-abinit-gene-0.0-mRNA-1	PRJEB506; PRJNA205202	EVPGVLRFG	Gly-loss +Amide	914.5338	76	84
flp-18	HCON_00164730; augustus-scaffold2866-abinit-gene-0.0-mRNA-1	PRJEB506; PRJNA205202	SMPGVLRFG	Gly-loss +Amide	904.4953	91	99
flp-18	HCON_00164730; augustus-scaffold2866-abinit-gene-0.0-mRNA-1	PRJEB506; PRJNA205202	SVPGVLRFG	Gly-loss +Amide	872.5232	102	110
flp-18	HCON_00164730; augustus-scaffold2866-abinit-gene-0.0-mRNA-1	PRJEB506; PRJNA205202	EMPGVLRFG	Gly-loss +Amide	946.5059	113	121
flp-18	HCON_00164730; augustus-scaffold2866-abinit-gene-0.0-mRNA-1	PRJEB506; PRJNA205202	AMPGVLRFG	Gly-loss +Amide	888.5004	124	132
flp-18	HCON_00164730; augustus-scaffold2866-abinit-gene-0.0-mRNA-1	PRJEB506; PRJNA205202	TEIPGMMRFG	Gly-loss +Amide	1079.526	135	144
flp-18	HCON_00164730; augustus-scaffold2866-abinit-gene-0.0-mRNA-1	PRJEB506; PRJNA205202	NVPGVLRFG	Gly-loss +Amide	899.5341	161	169
flp-19	HCOI00587500[b]	PRJEB506.WBPS10	WANQVRFG	Gly-loss +Amide	918.4824	50	57
flp-19	HCOI00587500[a]	PRJEB506.WBPS10	ASSWASSIRFG	Gly-loss +Amide	1109.562	60	70
flp-22	HCON_00012150	PRJEB506	TPSAKWMRFG	Gly-loss +Amide	1121.58	37	46
flp-22	HCON_00012150	PRJEB506	SPNAKWMRFG	Gly-loss +Amide	1134.576	49	58
flp-22	HCON_00012150	PRJEB506	TPDAKWMRFG	Gly-loss +Amide	1149.575	61	70
flp-24	HCON_00094680	PRJEB506	VPSAGDMMVRFG	Gly-loss +Amide	1207.584	53	64
flp-25	HCON_00078750; maker-scaffold165-snap-gene-0.6-mRNA-1	PRJEB506; PRJNA205202	HYDFVRFG	Gly-loss +Amide	981.4821	47	54
flp-25	HCON_00078750; maker-scaffold165-snap-gene-0.6-mRNA-1	PRJEB506; PRJNA205202	ASYDYIRFG	Gly-loss +Amide	1032.503	63	71
flp-33	HCON_00009870; maker-scaffold18501-snap-gene-0.8-mRNA-1	PRJEB506; PRJNA205202	SIDEIQKPRFG	Gly-loss +Amide	1230.672	66	76
flp-34	HCON_00140260; maker-scaffold19714-augustus-gene-0.9-mRNA-1	PRJNA205202	SDLSDFASAINSAGRLRYG	Gly-loss +Amide	1940.97	51	69

[a]The precursor name corresponds either to the one reported in project PRJEB506 or to the one described in project PRJNA205202 on the WormBase site. When sequences are predicted by both databases, the peptide sequence start and end positions refer to the database indicated first. [b]Denotes identified sequences from the PRJEB506 release (versions previous version 10).

SIRFG) whose sequences were removed from the updated versions of PRJEB506 were unambiguously identified in this study.

For peptides showing sequence discrepancies across those reported[14] and the WormBase data sets (Figure 1; Table 1), the use of a combination of all three data sets enabled sequence confirmation. For *flp-5*, *flp-7*, *flp-16*, and *flp-18*, the correct predicted sequences are those reported in the WormBase data sets. The peptide KHEYLRFSRG arising from *flp-14* and predicted only by the sequelogue database was not detected in this study, whereas the other *flp-14*-predicted peptide (KHEYLRFG) was unambiguously identified. This raises the question of the occurrence of the undetected peptide.

In addition to the confirmation that peptides were all amidated at the C-terminus, we also searched for additional processed peptides as described for *C. elegans*.[29] The authors looked for potential peptides derived from predicted neuropeptides precursors, which are flanked by (di)basic residues and which were not identified as mature peptides. Applying the same strategy to our *H. contortus* peptidomic data set, we could identify 14 additional peptides arising from 10 FLP precursors (Table 3). Here again, the interrogation of both worm databases led to the identification of the correct sequences for these additional peptides derived from *flp-5*, *flp-6*, *flp-15*, and *flp-17*.

For example, we found two additional non-FLP peptides encoded on *flp-17*, with one (AAEESAEIE) correctly predicted by both databases and the other (SAAEFDMPE) arising from the PRJEB506 database only. *Flp-6* gives rise to two additional non-FLP peptides (SDPELADQMMME and SSEVEDSPDAIDME) having the same predicted sequences on both databases: PRJEB506.WBPS14 and PRJNA205202.WBPS14. We also identified the peptide (SEAL**D**EDPMDVE) predicted only by the database PRJEB506.WBPS10 (version before the update). The PRJEB506.WBPS14 database predicted the sequence (SEAL**E**EDPMDVE), which was not identified in this study. Interestingly, the peptide (SSEVEDSPDAIDME) was wrongly predicted by the previous version, PRJEB506.WBPS10. Figure 2 shows the MS/MS spectra of the peptides SSEVEDSPDAIDME and SEALDEDPMDVE.

https://doi.org/10.1021/acsomega.1c00650
ACS Omega 2021, 6, 10288−10305

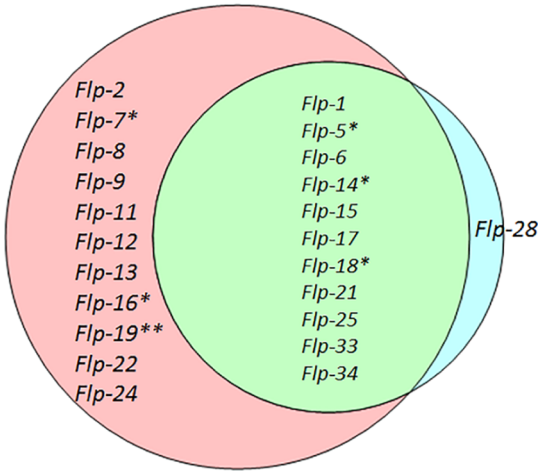

Figure 1. Presence of *flp*-gene sequences in the *H. contortus* databases reported in PRJEB506 (pink circle) and PRJNA205202 (blue circle) on WormBase (https://wormbase.org). *Flp-20*, *flp-23*, and *flp-32* were described by McCoy et al.[14] and *flp-32* by Atkinson et al.[35] * indicates discrepancies between sequences reported in McCoy et al.[14] and databases from Wormbase. ** *Flp-19* sequence was present in the previous PRJEB506 release (versions to 10) but not in versions 11−14.

Figure S1 illustrates different predicted *flp-6* sequence alignments.

All FLP precursor sequences identified in this study were aligned with the corresponding *C. elegans* FLP gene precursors (Figure S1). These alignments emphasize the strong homologies of bioactive peptides and their mono- and di-basic cleavage sites across nematode species, as highlighted.[14] This is illustrated in Figure 3 with the alignment of *flp-11* precursors for both *H. contortus* and *C. elegans*. The four amidated peptides observed for *C. elegans flp-11* were also detected for *H. contortus*, with one of them being amidated on a glutamine residue in both species. Compared to the studies of Van Bael et al.,[28,29] we were able to sequence the C-terminal peptide (SGHLDHIHDILSTLQKLQLANYH).

NLP Peptides. The identification of NLP peptides was carried out in association with the two PRJEB506 (version 10 and version 14) and PRJNA205202 WormBase data sets (there were no additional resources for NLP precursors as there was for FLP precursors). In addition, we performed a BLAST analysis of the 82 NLP precursors of *C. elegans* reported,[28,29] against the PRJEB506 and PRJNA205202 data sets. In total, 42 *nlp H. contortus* genes could be found using this BLAST approach (Table S1). Among these 42 *nlp* genes, 20 were predicted by both PRJNA205202 and PRJEB506 BioProjects and 22 were found only in the PRJEB506 data set. As noticed for FLP precursors, some NLP precursors (those from *nlp-1*, *nlp-19*, *nlp-35*, and *nlp-69*) were only predicted by the PRJEB506 versions before the update (versions 1−10), whereas *nlp-10*, *nlp-12*, and *nlp58* were found in the updated PRJEB506 versions (versions 11−14).

In this study, we clearly detected and identified 110 putative bioactive neuropeptides encoded by 33 of these 42 predicted NLP precursors (Table 4). We also identified three additional peptides arising from the precursor HCON_00135420 (PRJEB506 nomenclature), which could not be assigned by BLAST searches to any *C. elegans* precursor.

Table 3. *flp*-Gene-Encoded Non-FLP Peptides Identified in the First-Stage (L1) and Third-Stage Larvae (L3) of *H. contortus*

gene	precursor name[a]	database	sequence	modifications	mass	start position[b]	end position[b]
flp-2	HCON_00188000	PRJEB506	GPMFEPYFDY	unmodified	1264.511	61	70
flp-5	HCON_00164350	PRJEB506	SGTNTWDDDSSDITSYAHQDD	unmodified	2328.889	57	77
flp-6	HCON_00155670; augustus-scaffold18780-abinit-gene-0.3-mRNA-1	PRJEB506; PRJNA205202	SDPELADQMMME	unmodified	1395.536	41	52
flp-6	HCON_00155670	PRJEB506	SEALDEDPMDVE	unmodified	1348.534	65	76
flp-6	HCON_00155670; augustus-scaffold18780-abinit-gene-0.3-mRNA-1	PRJEB506; PRJNA205202	SSEVEDSPDAIDME	unmodified	1522.598	99	112
flp-11	HCON_00176100	PRJEB506	SGHLDHIHDILSTLQKLQLANYH	unmodified	2652.377	86	108
flp-13	HCON_00095850	PRJEB506	VDTLSRES	unmodified	905.4454	35	42
flp-15	U6PJU1 CBN-FLP-15protein GN=HCOI 01474400	PRJEB506	EIEDITDDSK	unmodified	1163.519	22	31
flp-15	U6PJU1 CBN-FLP-15protein GN=HCOI 01474400	PRJEB506	STFDYPTVFDQQPYYYFV	unmodified	2279.01	64	81
flp-17	HCON_00123460; maker-C469629-augustus-gene-0.17-mRNA-1	PRJEB506; PRJNA205202	AAEESAEIE	unmodified	947.4084	82	90
flp-17	maker-C469629-augustus-gene-0.17-mRNA-1	PRJNA205202	SAAEFDMPE	unmodified	995.3906	102	110
flp-18	HCON_00164730; augustus-scaffold2866-abinit-gene-0.0-mRNA-1	PRJEB506; PRJNA205202	STYDTIPLELLD	unmodified	1378.687	147	148
flp-25	HCON_00078750; maker-scaffold165-snap-gene-0.6-mRNA-1	PRJEB506; PRJNA205202	SQIDSDDLNARFSPYQFL	unmodified	2114.991	74	91
flp-33	HCON_00009870; maker-scaffold18501-snap-gene-0.8-mRNA-1	PRJEB506; PRJNA205202	SPLEGFEDISSMM	unmodified	1441.611	52	64

[a]The precursor name corresponds either to the one reported in project PRJEB506 or to the one described in project PRJNA205202 on the WormBase site. [b]When sequences are predicted by both databases, the peptide sequence start and end positions refer to the database indicated first.

https://doi.org/10.1021/acsomega.1c00650
ACS Omega 2021, 6, 10288−10305

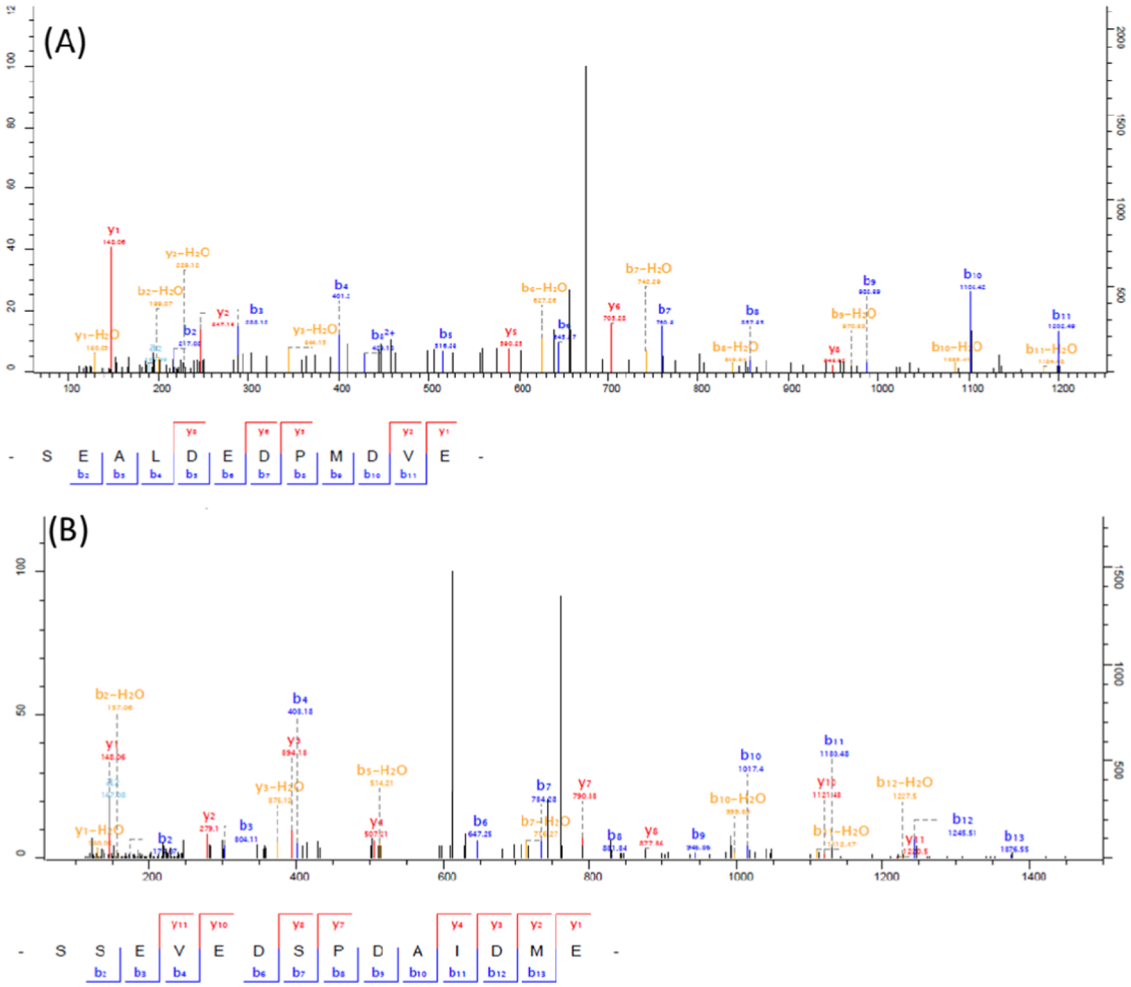

Figure 2. MS/MS spectra of two unmodified peptides of the *H. contortus flp-6*. The fragmentation schemes enabled the identification of the peptide SEALDEDPMDVE in the WormBase, PRJEB506.WBPS10 database analysis (A), and of the peptide SSEVEDSPDAIDME upon the analysis of both PRJEB506.WBPS14 and PRJNA205202.WBPS14 WormBase (B).

HCON_00176100
SP|Q21156|FLP11_CAEEL

```
MTSSTTIKFCIIAVVI-ASLRAQDSFALEKRAMRNALVRFGRAGGSMRNALVRFGKRYLA 59
MTQFSALALLLIVFVAASFAQSYDDVSAEKRAMRNALVRFGRASGGMRNALVRFGKRSPL 60
**. ::: : :*..*  :  :: *..: ***************.*.***********

TDDDYAT-AAAQGKRNGAPQPFVRFGRSGHLDHIHDILSTLQKLQLANYH 108
DEEDFAPESPLQGKRNGAPQPFVRFGRSGQLDHMHDLLSTLQKLKFANNK 110
::*:*  :  ******************:***:**:*******::** :
```

Figure 3. Sequence alignments of *H. contortus flp-11* (sequence in the BioProject PRJEB506 protein fasta file, Wormbase source) with *C. elegans flp-11* (UniProtKB source). Sequences were aligned using the Clustal Omega program (http://www.clustal.org). Predicted signal peptide is indicated in italics. Putative mono- and di-basic cleavage sites are shown in red. The potential C-terminal glycine residues for amidation are indicated in brown. *C. elegans* peptide data shown in the study of Van Bael et al.[29] are highlighted in blue. *H. contortus* FLP peptide sequences identified in this study are shown in bold green with the sequence of the unmodified peptides being underlined. The amidated glutamine residues identified in both species are indicated in purple.

As seen for FLP peptides, the use of the two WormBase data sets (PRJEB506 versions 10 and 14, and PRJNA205202) yielded an increase in the number of identified NLP peptides and allowed us to inform the predicted sequences where discrepancies existed between databases, as shown for *nlp-5, nlp-7, nlp-15, nlp-9, nlp-13*, and *nlp-18* (Table 4; Figure S2). Detection of the peptide GGGRAFFGGWQPYESLGARMD encoded on *nlp-9* shows that the correct sequence was the one predicted in PRJNA205202, whereas for *nlp-7*, nlp-13, *nlp-15, nlp-18*, and one peptide of *nlp-5*, the correct sequences were predicted in PRJEB506. More surprising was the fact that we clearly identified both of the WormBase predicted sequences for the C-terminal peptide of *nlp-5* (SRLFSTYYYLPYRD-SLEDMDQNAQE, predicted in PRJNA205202, and SRLFSTYYYLPYRDSLEDMDQNVQE, predicted in

https://doi.org/10.1021/acsomega.1c00650
ACS Omega 2021, 6, 10288−10305

Table 4. NLP Peptides Identified in the First-Stage (L1) and Third-Stage Larvae (L3) of *H. contortus*

NLP	precursor name[a]	database	sequence	modifications	mass	start position[b]	end position[b]
nlp-1[c]	HCOI00158100	PRJEB506.WBPS10	AVMFPRTFGALFG	Gly-loss+Amide	1354.722	31	43
nlp-1[c]	HCOI00158100	PRJEB506.WBPS10	MDMKHYFVGLG	Gly-loss+Amide	1238.594	82	92
nlp-3	HCON_00188680	PRJEB506	AINPFLDSMG	Gly-loss+Amide	1005.495	28	37
nlp-3	HCON_00188680	PRJEB506	AVNPFLDSFG	Gly-loss+Amide	1007.508	40	49
nlp-3	HCON_00188680	PRJEB506	SSRYQPYYHLD	unmodified	1427.647	52	62
nlp-3	HCON_00188680	PRJEB506	YFDSLAGQALG	Gly-loss+Amide	1082.54	65	75
nlp-5	HCON_00046600; maker-C469189-snap-gene-0.14-mRNA-1	PRJEB506; PRJNA205202	ALSSFDTLGGIGLG	Gly-loss+Amide	1248.671	42	55
nlp-5	HCON_00046600	PRJEB506	TQLSSIDSLGGLGLG	Gly-loss+Amide	1358.741	46	60
nlp-5	HCON_00046600; maker-C469189-snap-gene-0.14-mRNA-1	PRJEB506; PRJNA205202	SEDTAKKALSSFDTLGGIGLG	Gly-loss+Amide	2008.048	123	143
nlp-5	HCON_00046600; maker-C469189-snap-gene-0.14-mRNA-1	PRJEB506; PRJNA205202	DDMLAGEKKSVSSFDTLAGIGLG	Gly-loss+Amide	2252.136	146	168
nlp-5	maker-C469189-snap-gene-0.14-mRNA-1	PRJNA205202	SRLFSTYYYLPYRDSLEDMDQNAQE	unmodified	3103.387	171	195
nlp-5	HCON_00046600	PRJEB506	SRLFSTYYYLPYRDSLEDMDQNVQE	unmodified	3131.418	127	151
nlp-7	HCON_00165470; maker-C452207-snap-gene-0.3-mRNA-1	PRJEB506; PRJNA205202	LVIPSYLSSHYD	unmodified	1392.693	32	43
nlp-7	HCON_00165470; maker-C452207-snap-gene-0.3-mRNA-1	PRJEB506; PRJNA205202	TLDFDDPRLFSTAFG	Gly-loss+Amide	1642.799	46	60
nlp-7	HCON_00165470; maker-C452207-snap-gene-0.3-mRNA-1	PRJEB506; PRJNA205202	NGLVTTTLNRPRFI	unmodified	1600.905	63	76
nlp-7	HCON_00165470; maker-C452207-snap-gene-0.3-mRNA-1	PRJEB506; PRJNA205202	SPFLGTNVGLAYI	unmodified	1350.718	79	91
nlp-7	HCON_00165470; maker-C452207-snap-gene-0.3-mRNA-1	PRJEB506; PRJNA205202	ADMDPRFISNSFG	Gly-loss+Amide	1397.64	94	106
nlp-7	HCON_00165470; maker-C452207-snap-gene-0.3-mRNA-1	PRJEB506; PRJNA205202	STLYDFDDPRFASLSFG	Gly-loss+Amide	1878.879	109	125
nlp-7	HCON_00165470; maker-C452207-snap-gene-0.3-mRNA-1	PRJEB506; PRJNA205202	SGFDFDDPRFSSMSFG	Gly-loss+Amide	1739.725	128	143
nlp-7	HCON_00165470; maker-C452207-snap-gene-0.3-mRNA-1	PRJEB506; PRJNA205202	SGFDLEDPRFASMSFG	Gly-loss+Amide	1703.761	146	161
nlp-7	HCON_00165470; maker-C452207-snap-gene-0.3-mRNA-1	PRJEB506; PRJNA205202	SGFN FEDPRFASLSFG	Gly-loss+Amide	1718.805	164	179
nlp-7	HCON_00165470; maker-C452207-snap-gene-0.3-mRNA-1	PRJEB506; PRJNA205202	SGFDLDDPRFASMSFG	Gly-loss+Amide	1689.746	182	197
nlp-7	HCON_00165470	PRJEB506	SGSDLEDPRYWSMSFG	Gly-loss+Amide	1774.762	200	215
nlp-8	HCON_00010710; maker-scaffold14524-snap-gene-0.4-mRNA-1	PRJEB506; PRJNA205202	AFDRIESN DFGLF	unmodified	1529.715	49	61
nlp-8	HCON_00010710; maker-scaffold14524-snap-gene-0.4-mRNA-1	PRJEB506; PRJNA205202	AFDRIEMADFGF	unmodified	1417.634	69	80
nlp-8	HCON_00010710; maker-scaffold14524-snap-gene-0.4-mRNA-1	PRJEB506; PRJNA205202	AFDRVGRTEFGFEGVL	unmodified	1798.9	85	100
nlp-8	HCON_00010710; maker-scaffold14524-snap-gene-0.4-mRNA-1	PRJEB506; PRJNA205202	TEFGFEGVL	unmodified	997.4757	92	100
nlp-8	HCON_00010710; maker-scaffold14524-snap-gene-0.4-mRNA-1	PRJEB506; PRJNA205202	AADRLADIGFRN	unmodified	1317.679	104	115

https://doi.org/10.1021/acsomega.1c00650
ACS Omega 2021, 6, 10288−10305

Table 4. continued

NLP	precursor name[a]	database	sequence	modifications	mass	start position[b]	end position[b]
nlp-9	HCON_00136940; maker-scaffold10126-snap-gene-0.11-mRNA-1	PRJEB506; PRJNA205202	GGARAFHGYFNMPSS	unmodified	1597.71	48	62
nlp-9	HCON_00136940; maker-scaffold10126-snap-gene-0.11-mRNA-1	PRJEB506; PRJNA205202	LSGEYPYYLYE	unmodified	1395.623	65	75
nlp-9	maker-scaffold10126-snap-gene-0.11-mRNA-1	PRJNA205202	GGGRAFFGGWQPYESLGARMD	unmodified	2258.033	78	98
nlp-9	HCON_00136940; maker-scaffold10126-snap-gene-0.11-mRNA-1	PRJEB506; PRJNA205202	SSSLWEFLEDRNAL	unmodified	1665.8	127	140
nlp-10	HCON_00073270; maker-scaffold13486-augustus-gene-0.18-mRNA-	PRJEB506; PRJNA205202	AVMPFSGGLYG	Gly-loss+Amide	1039.516	64	74
nlp-10	HCON_00073270; maker-scaffold13486-augustus-gene-0.18-mRNA-	PRJEB506; PRJNA205202	SEMPDDMYIERPVLPLSAGWQE	unmodified	2562.177	90	111
nlp-10	HCON_00073270; maker-scaffold13486-augustus-gene-0.18-mRNA-	PRJEB506; PRJNA205202	AVMPFSGGLYGKRAVMPFSGGLYG	Gly-loss+Amide	2403.223	114	137
nlp-10	HCON_00073270; maker-scaffold13486-augustus-gene-0.18-mRNA-	PRJEB506; PRJNA205202	AAMPFSGGLYG	Gly-loss+Amide	1011.485	140	150
nlp-10	HCON_00073270; maker-scaffold13486-augustus-gene-0.18-mRNA-	PRJEB506; PRJNA205202	ADRYIRSPMPISGGIFG	Gly-loss+Amide	1777.93	153	169
nlp-10	HCON_00073270; maker-scaffold13486-augustus-gene-0.18-mRNA-	PRJEB506; PRJNA205202	SPMPISGGIFG	Gly-loss+Amide	1003.516	159	169
nlp-11	HCON_00062360; augustus-C472037-abinit-gene-0.0-mRNA-1	PRJEB506; PRJNA205202	LETELHPLVMGMYGFGPENNAY	unmodified	2481.135	36	57
nlp-11	HCON_00062360; augustus-C472037-abinit-gene-0.0-mRNA-1	PRJEB506; PRJNA205202	HISPSFDVEEDVGNMRTLMDIG	Gly-loss+Amide	2403.12	67	88
nlp-11	HCON_00062360; augustus-C472037-abinit-gene-0.0-mRNA-1	PRJEB506; PRJNA205202	QLSVADDVGRQMQMYHRLFEAG	Gly-loss+Amide	2492.205	91	112
nlp-11	HCON_00062360; augustus-C472037-abinit-gene-0.0-mRNA-1	PRJEB506; PRJNA205202	AALSPSQDLQSAVELSNYLERAG	Gly-loss+Amide	2360.197	116	138
nlp-12	HCON_00021180; maker-scaffold5805-snap-gene-0.2-mRNA-1	PRJEB506; PRJNA205202	DYRPLQFG	Gly-loss+Amide	936.4818	31	38
nlp-12	HCON_00021180; maker-scaffold5805-snap-gene-0.2-mRNA-1	PRJEB506; PRJNA205202	DGYRPLQFG	Gly-loss+Amide	993.5032	41	49
nlp-12	HCON_00021180; maker-scaffold5805-snap-gene-0.2-mRNA-1	PRJEB506; PRJNA205202	SPLASAFLVPAL	unmodified	1184.681	62	73
nlp-13	HCON_00136950; maker-C471727-snap-gene-0.19-mRNA-1	PRJEB506; PRJNA205202	NDFSRDIMHFG	Gly-loss+Amide	1279.577	33	43
nlp-13	HCON_00136950; maker-C471727-snap-gene-0.19-mRNA-1	PRJEB506; PRJNA205202	AYGNGRLVAYGGPAFERDMMAFG	Gly-loss+Amide	2391.125	46	68
nlp-13	HCON_00136950; maker-C471727-snap-gene-0.19-mRNA-1	PRJEB506; PRJNA205202	SGGFEREMMSFG	Gly-loss+Amide	1275.538	71	82
nlp-13	HCON_00136950	PRJEB506	SPFEREFLSFG	Gly-loss+Amide	1256.61E	85	95
nlp-13	HCON_00136950; maker-C471727-snap-gene-0.19-mRNA-1	PRJEB506; PRJNA205202	GSEFDREMLSFG	Gly-loss+Amide	1315.587	98	109
nlp-13	HCON_00136950; maker-C471727-snap-gene-0.19-mRNA-1	PRJEB506; PRJNA205202	DEFERSMMAFG	Gly-loss+Amide	1260.527	112	122
nlp-14	HCON_00190000; maker-scaffold4554-snap-gene-0.8-mRNA-1	PRJEB506; PRJNA205202	ALDSLEGDGFGGLF	unmodified	1396.651	52	65
nlp-14	HCON_00190000; maker-scaffold4554-snap-gene-0.8-mRNA-1	PRJEB506; PRJNA205202	SLDSLEGDGFGFD	unmodified	1357.567	68	80

https://doi.org/10.1021/acsomega.1c00650
ACS Omega 2021, 6, 10288−10305

Table 4. continued

NLP	precursor name[a]	database	sequence	modifications	mass	start position[b]	end position[b]
nlp-14	HCON_00190000; maker-scaffold4554-snap-gene-0.8-mRNA-1	PRJEB506; PRJNA205202	ALNALDGTGFGFD	unmodified	1296.599	83	95
nlp-14	HCON_00190000; maker-scaffold4554-snap-gene-0.8-mRNA-1	PRJEB506; PRJNA205202	ALNSLEGTGFGFD	unmodified	1326.609	98	110
nlp-14	HCON_00190000; maker-scaffold4554-snap-gene-0.8-mRNA-1	PRJEB506; PRJNA205202	SLNSIEGTGFGFD	unmodified	1342.604	113	125
nlp-14	HCON_00190000; maker-scaffold4554-snap-gene-0.8-mRNA-1	PRJEB506; PRJNA205202	SLDSTEGTGFGYRRG	Gly-loss+Amide	1543.738	160	174
nlp-14	HCON_00190000; maker-scaffold4554-snap-gene-0.8-mRNA-1	PRJEB506; PRJNA205202	TLPQITGTHPYLRLY	unmodified	1771.962	177	191
nlp-15	HCON_00024600; maker-C472057-snap-gene-0.5-mRNA-1	PRJEB506; PRJNA205202	AFDSLSGSGLTPFN	unmodified	1411.662	47	60
nlp-15	HCON_00024600; maker-C472057-snap-gene-0.5-mRNA-1	PRJEB506; PRJNA205202	AFDSLAGSGFTGFD	unmodified	1390.604	79	92
nlp-15	HCON_00024600	PRJEB506	SPIALNGGYYQPLREDALLL	unmodified	2202.169	95	114
nlp-17	HCON_00114940	PRJEB506	NSLSN MMRLG	Gly-loss+Amide	1063.527	44	49
nlp-17	HCON_00114940	PRJEB506	VDALKEQEPCVDCSLGNLMRLG	2 Cys-Cys; Gly-loss+	2329.123	52	73
nlp-18	HCON_00035340; augustus-scaffold7830-abinit-gene-0.1-mRNA-1	PRJEB506; PRJNA205202	SDEVVEDDGELE	unmodified	1334.536	52	63
nlp-18	HCON_00035340; augustus-scaffold7830-abinit-gene-0.1-mRNA-1	PRJEB506; PRJNA205202	SPYRQFAFA	unmodified	1085.529	74	82
nlp-18	HCON_00035340	PRJEB506	GSPYGFAFA	unmodified	915.4127	85	93
nlp-19[c]	HCOI00354200	PRJEB506.WBPS10	IGMRLPNIIYM	unmodified	1319.709	52	62
nlp-20	HCON_00131138	PRJEB506	DLDNSKKFSFA	unmodified	1270.619	64	74
nlp-20	HCON_00131138	PRJEB506	FADRDDRLIR	unmodified	1275.668	105	114
nlp-21	HCON_00067330; maker-C471673-augustus-gene-0.17-mRNA-1	PRJEB506; PRJNA205202	GGGRAFVPIEE	unmodified	1130.572	27	37
nlp-21	HCON_00067330; maker-C471673-augustus-gene-0.17-mRNA-1	PRJEB506; PRJNA205202	GGARAFFGDE	unmodified	1025.457	39	48
nlp-21	HCON_00067330; maker-C471673-augustus-gene-0.17-mRNA-1	PRJEB506; PRJNA205202	GGARAFVVDT	unmodified	991.5087	51	60
nlp-21	HCON_00067330; maker-C471673-augustus-gene-0.17-mRNA-1	PRJEB506; PRJNA205202	GGGRAFLPVEE	unmodified	1130.572	73	83
nlp-21	HCON_00067330; maker-C471673-augustus-gene-0.17-mRNA-1	PRJEB506; PRJNA205202	GGARAFFKDD	unmodified	1082.515	85	94
nlp-21	HCON_00067330; maker-C471673-augustus-gene-0.17-mRNA-1	PRJEB506; PRJNA205202	GGARAFVPVKEEDEGQSFTDLE	unmodified	2380.118	97	118
nlp-21	HCON_00067330; maker-C471673-augustus-gene-0.17-mRNA-1	PRJEB506; PRJNA205202	GGARAFFVP	unmodified	920.4868	121	129
nlp-21	HCON_00067330; maker-C471673-augustus-gene-0.17-mRNA-1	PRJEB506; PRJNA205202	GGARAFFVPK	unmodified	1048.582	121	130
nlp-21	HCON_00067330; maker-C471673-augustus-gene-0.17-mRNA-1	PRJEB506; PRJNA205202	GGGRAFLPIEE	unmodified	1144.588	132	142
nlp-21	HCON_00067330; maker-C471673-augustus-gene-0.17-mRNA-1	PRJEB506; PRJNA205202	GGARAFFQEP	unmodified	1078.52	144	153
nlp-21	HCON_00067330; maker-C471673-augustus-gene-0.17-mRNA-1	PRJEB506; PRJNA205202	GGARAFP	unmodified	674.35	156	162

https://doi.org/10.1021/acsomega.1c00650
ACS Omega 2021, 6, 10288−10305

Table 4. continued

NLP	precursor name[a]	database	sequence	modifications	mass	start position[b]	end position[b]
nlp-21	HCON_00067330; maker-C471673-augustus-gene-0.17-mRNA-1	PRJEB506; PRJNA205202	GGGRAFVPQ	unmodified	887.4614	165	173
nlp-24	HCON_00126360	PRJEB506	VNPLQGAMMGAMMGAMRG	Gly-loss+Amide	1763.813	66	83
nlp-31	HCON_00105250	PRJEB506	PVVVERTIIYPG	Gly-loss+Amide	1283.76	68	79
nlp-35[c]	HCOI00356900; snap-scaffold16547-abinit-gene-0.6-mRNA-1	PRJEB506.WBPS10; PRJNA205202	DQLAFSGQNAYLRQLLQN LKPK	unmodified	2544.381	46	67
nlp-37	HCON_00163850	PRJEB506	NNAEVVNHILKNFGTLDRLGDVG	Gly-loss+Amide	2436.287	60	83
nlp-40	HCON_00017810.1; maker-C461709-augustus-gene-0.1-mRNA-1	PRJEB506; PRJNA205202	QLTAPTTMEKEEA	Gln->pyro-Glu	1430.66	41	53
nlp-40	HCON_00017810.1; maker-C461709-augustus-gene-0.1-mRNA-1	PRJEB506; PRJNA205202	MVAWQPM	unmodified	861.3877	67	73
nlp-42	HCON_00142640	PRJEB506	SAVGELSYPRRFL	unmodified	1493.799	36	48
nlp-42[c]	HCOI01162100	PRJEB506.WBPS10	SVDWHSLGWAWG	Gly-loss+Amide	1341.626	57	68
nlp-44	HCON_00163905	PRJEB506	STLPLSSLLVPYPRVG	Gly-loss+Amide	1639.966	34	49
nlp-44	HCON_00163905	PRJEB506	SFFTGDRNVYPPTSI	unmodified	1699.821	52	66
nlp-44	HCON_00163905	PRJEB506	RYLYTARVG	Gly-loss+Amide	1039.593	79	87
nlp-54	HCON_00096380	PRJEB506	GNM WGTPSKSYGYTN LA E	unmodified	1974.878	43	60
nlp-58	HCON_00137190	PRJEB506	SLYGVDDGFTFKGFRGL	unmodified	1877.931	41	57
nlp-58	HCON_00163905	PRJEB506	MPYMNLKGLRG	Gly-loss+Amide	1220.652	62	72
nlp-59	HCON_00096380; maker-scaffold14296-augustus-gene-0.22-mRNA-1	PRJEB506; PRJNA205202	FEGLADYVALEDPNA	unmodified	1622.746	63	77
nlp-59	HCON_00096380; maker-scaffold14296-augustus-gene-0.22-mRNA-1	PRJEB506; PRJNA205202	LAILSARGFG	Gly-loss+Amide	945.576	85	94
nlp-67	HCON_00186320; maker-scaffold993-snap-gene-0.2-mRNA-	PRJEB506; PRJNA205202	AVPVEVEQRE	unmodified	1154.593	54	63
nlp-67	HCON_00186320; maker-scaffold993-snap-gene-0.2-mRNA-	PRJEB506; PRJNA205202	SYPRNCYFSPIQCLFT	2 Cys-Cys	1935.865	71	86
nlp-68	HCON_00070810; augustus-scaffold17454-abinit-gene-0.0-mRNA-1	PRJEB506; PRJNA205202	LVREPPLI	unmodified	935.5804	50	57
nlp-68	HCON_00070810; augustus-scaffold17454-abinit-gene-0.0-mRNA-1	PRJEB506; PRJNA205202	GIDPFSIPTLIKEPPL	unmodified	1735.976	60	75
nlp-68	HCON_00070810; augustus-scaffold17454-abinit-gene-0.0-mRNA-1	PRJEB506; PRJNA205202	DSYVYPSTNSQLSDRIPLREPPL	unmodified	2646.329	82	104
nlp-69[c]	HCOI01768700	PRJEB506.WBPS10	FYRTGGTILLG	Gly-loss+Amide	1138.65	58	68
nlp-71	HCON_00122860	PRJEB506	ALNQFKNCYFSPIQCVLME	2 Cys-Cys	2245.037	62	80
nlp-74	HCON_00082180; maker-scaffold4879-augustus-gene-0.4-mRNA-1	PRJEB506; PRJNA20222	APQMYDDVQFV	unmodified	1311.581	28	38
nlp-74	HCON_00082180; maker-scaffold4879-augustus-gene-0.4-mRNA-1	PRJEB506; PRJNA205202	SNAELINGLIGMDLGKLSAVG	Gly-loss+Amide	2013.093	41	61
nlp-74	HCON_00082180; maker-scaffold4879-augustus-gene-0.4-mRNA-1	PRJEB506; PRJNA205202	SNAELINGLLGMNLNKLSSAG	Gly-loss+Amide	2057.094	64	84
nlp-81	HCON_00107730	PRJEB506	FTNGDFFVP	unmodified	1101.524	48	56
nlp-81	HCON_00107730	PRJEB506	WIPSGGAGLVSGRG	unmodified	1312.689	60	73
nlp-81	HCON_00107730	PRJEB506	DWRSAIAEPNF	unmodified	1304.615	83	93
HCON_00135420	HCON_00135420; maker-scaffold6512-augustus-gene-0.7-mRNA-1	PRJEB506; PRJNA205202	ARNPYSWMVVDQS	unmodified	1551.714	45	57

https://doi.org/10.1021/acsomega.1c00650
ACS Omega 2021, 6, 10288−10305

Table 4. continued

NLP	precursor name[a]	database	sequence	modifications	mass	start position[b]	end position[b]
HCON_00135420	HCON_00135420; maker-scaffold6512-augustus-gene-0.7-mRNA-1	PRJEB506	SRNPYSWMVHSKG	Gly-loss+Amide	1489.725	60	72
HCON 00135420	HCON_00135420; maker-scaffold6512-augustus-gene-0.7-mRNA-1	PRJEB506; PRJNA205202	ARNPYSWMNE	unmodified	1266.545	101	110

[a]The precursor name corresponds either to the one reported in project PRJEB506 or to the one reported in project PRJNA205202 on the WormBase site. [b]When sequences are predicted by both databases, the peptide sequence start and end positions refer to the database indicated first. [c]Denotes identified sequences from the PRJEB506 release (versions to 10).

PRJEB506); the corresponding MS/MS spectra are shown in Figure 4.

All *H. contortus* NLP sequences revealed in this study were aligned with their *C. elegans* homologues as shown in Figure S2. As reported for *C. elegans*,[28,29] we also detected equivalent unrecorded *H. contortus* neuropeptides for *nlp-3*, *nlp-9*, *nlp-10*, and *nlp-12* (these peptides are underlined in Figure S2). As already shown for FLP peptides, these alignments emphasize the similarity in neuropeptide sequences between both *C. elegans* and *H. contortus* with the identification of peptides bearing the C-terminal glycine residue for amidation and with peptides not modified but being flanked by di- or mono-basic residues. In this study, we were able to isolate and identify peptides arising from *nlp-17, nlp-19, nlp-44, nlp-54, nlp-59, nlp-67, nlp-38, nlp-69*, and *nlp-71* that were not previously reported in similar studies on *C. elegans*. Of particular interest are the C-terminal peptides of *nlp-17*, *nlp-67*, and *nlp-71*, which were unambiguously identified with one disulfide bridge, as shown by their MS/MS spectra (Figure 5). The study on *C. elegans*[28,29] reported the homologous sequences with the prediction of disulfide bridges, but there was no biochemical isolation or characterization.

Label-Free Quantification of Neuropeptides. Neuropeptide quantification was performed on four L1 and three L3 biological replicates. Normalized intensities measured for all identified peptides arising from predicted neuropeptide precursors are listed in Table S2.

Relative Abundance of Endogenous Peptides. Some of the detected peptides are shorter versions of the same peptide, likely reflecting the degradation of bioactive peptides during sample processing. We calculated the intensities of truncated forms and compared these to the intensity of the corresponding nontruncated bioactive peptides. On average, we found that these degraded forms represented less than 15% of the entire form, indicative of a low level of peptide degradation. It is noteworthy that for most amidated peptides, we also detected two other minor forms, representing less than 5% of the mature peptide, one corresponding to the nonamidated peptide and the second one corresponding to the substrate of the amidating enzymes, which act sequentially on C-terminal Glycine-extended immature peptides (Table S2).

The relative abundance of all endogenous peptides reported in Tables 2 and 4 is shown in Figure 7, spanning four orders of magnitude both in the L1 and L3 life stages. Among the 181 detected bioactive peptides, the most intense *flp* and *nlp* peptides quantified are indicated in Figure 6.

Differential Neuropeptide Expression between L1 Stage and L3 Stage Larvae of H. contortus. We compared the relative peptide expression in L1 (free-living stage) and L3 (infective) life stages for the 181 identified mature peptides (Table S3). All resulting individual boxplots are depicted in Figure S3. Based on an arbitrary fold-change of 3 and a *p*-value of 0.01, we found 29 peptides more highly expressed in L3s and 22 more highly expressed in L1s (Figure 7).

Data shown in Table S2 and Figure S3 highlight that peptides arising from the same precursor can either follow the same trend or vary greatly in expression between L1 and L3 worms. For example, all four *nlp-3* peptides (AINPFLDSMG, AVNPFLDSFG, SSRYQPYYHLD, and YFDSLAGQALG) are more highly expressed in L3s (Figure 8A), whereas *nlp-10* has two peptides (AVMPFSGGLYG and ADRYIRSMPISGGIFG)

https://doi.org/10.1021/acsomega.1c00650
ACS Omega 2021, 6, 10288−10305

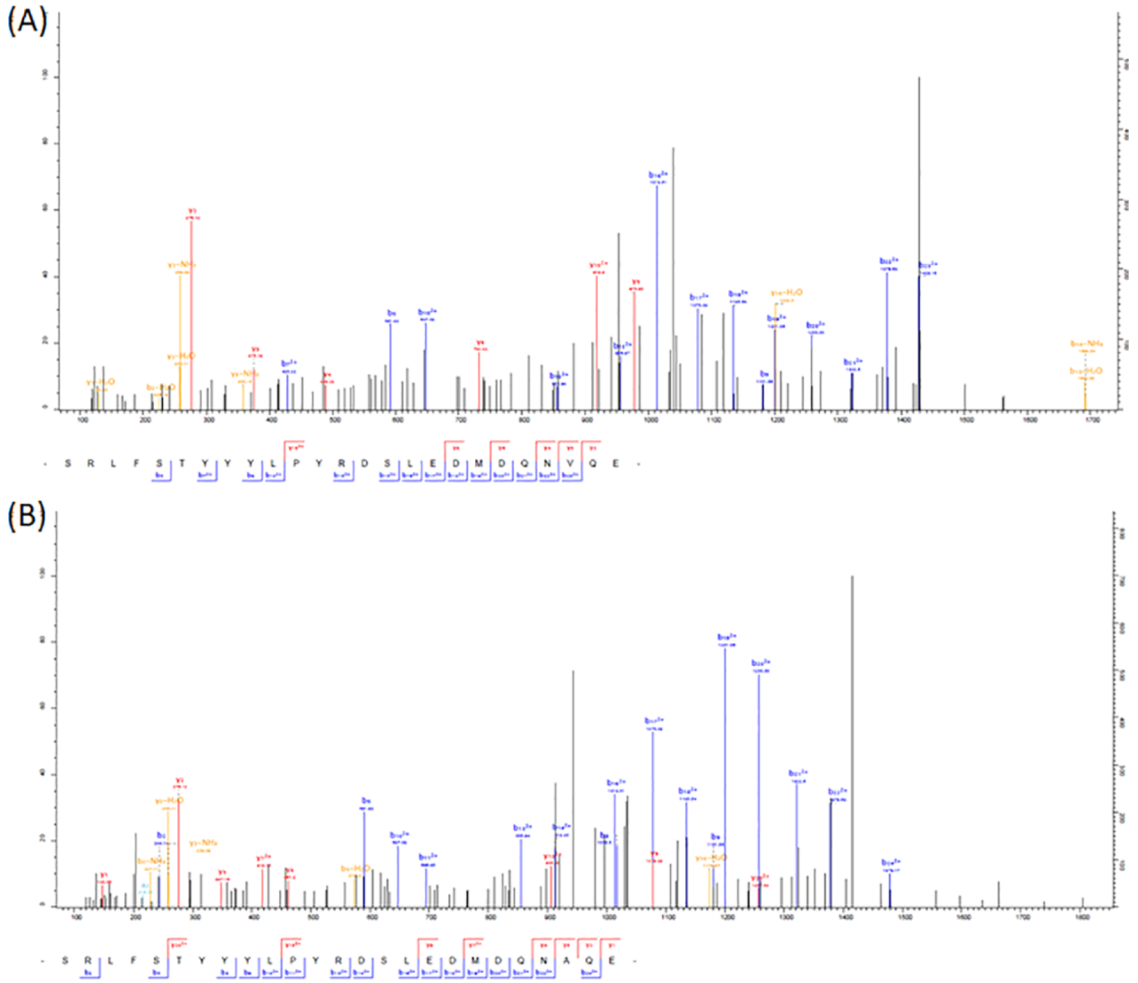

Figure 4. MS/MS spectra of two peptides of the *H. contortus* neuropeptide precursor encoded by *nlp*-5. The fragmentation schemes allowed the identification of the peptide SRLFSTYYYLPYRDSLEDMDQNVQE from the WormBase PRJEB506 data set analysis (A) and of the peptide SRLFSTYYYLPYRDSLEDMDQNAQE from analysis of the WormBase PRJNA205202 data set (B).

that show opposite trends in the two life stages, being lower in the L3 stage worms (Figure 8B).

DISCUSSION

The present study is the first whole-parasitic peptidome analysis of *H. contortus*. Previously, only two FLP neuropeptides have been directly sequenced for this nematode.[31,32] These new findings enhance the understanding of nematode neuropeptide biology and enhance the FLP-activated G-protein coupler receptors profiling described in McCoy et al.[14]

This is also one of the most comprehensive neuropeptidome analyses of a nematode with a total of 181 peptides (68 FLPs and 113 NLPs) being identified biochemically using MS/MS. It can be compared with similar studies performed on *C. elegans*, which led to the identification of 203 neuropeptides based on mass matching,[28,29] 131 among them with sequenced levels using LC-MS/MS. In our study, all of the identified peptides were fully sequenced by MS/MS. However, five predicted FLP and nine NLP precursors remain undetected in this study. This can be due to various reasons. At first, it is not possible to anticipate which predicted peptides will be expressed and correctly processed into bioactive peptides. Another possibility is that some neuropeptides may be present in other developmental stages or may be expressed under certain conditions. In addition, we cannot exclude experimental bias like neuropeptide degradation during sample processing, leading to low-molecular-weight peptides not detectable by LC/MS. The stochastic precursor selection of DDA may also lead to inconsistent detection of peptides, and finally, some neuropeptides are certainly below the current detection threshold of MS due to their weak expression.

The results obtained from *H. contortus* larvae peptidomics profiling reveal and expand on the known complexity of neuropeptide expression in nematodes. These data are consistent with nematode parasites, displaying remarkable neuropeptide complexity despite their apparent nervous system simplicity.[37] The data further confirm that peptide-based neuronal signaling in parasitic nematodes is similarly complex to that reported for free-living nematodes, at least in these clade V nematodes. This is not surprising considering that *H. contortus* has both free-living and parasitic stages and the L3 stage transitions from the free-living to a host-based environment.

In this study, the differentially expressed neuropeptides between two key developmental stages of *H. contortus* (the first-larval stage, L1, and the infective stage, L3) were investigated by comparative peptidomics. The free-living stage L1 is motile and exits the egg to feed on feces, while the L3 stage waits in water droplets on vegetation and enters a resting stage that relies on reserves, slows its metabolic rate,

https://doi.org/10.1021/acsomega.1c00650
ACS Omega 2021, 6, 10288−10305

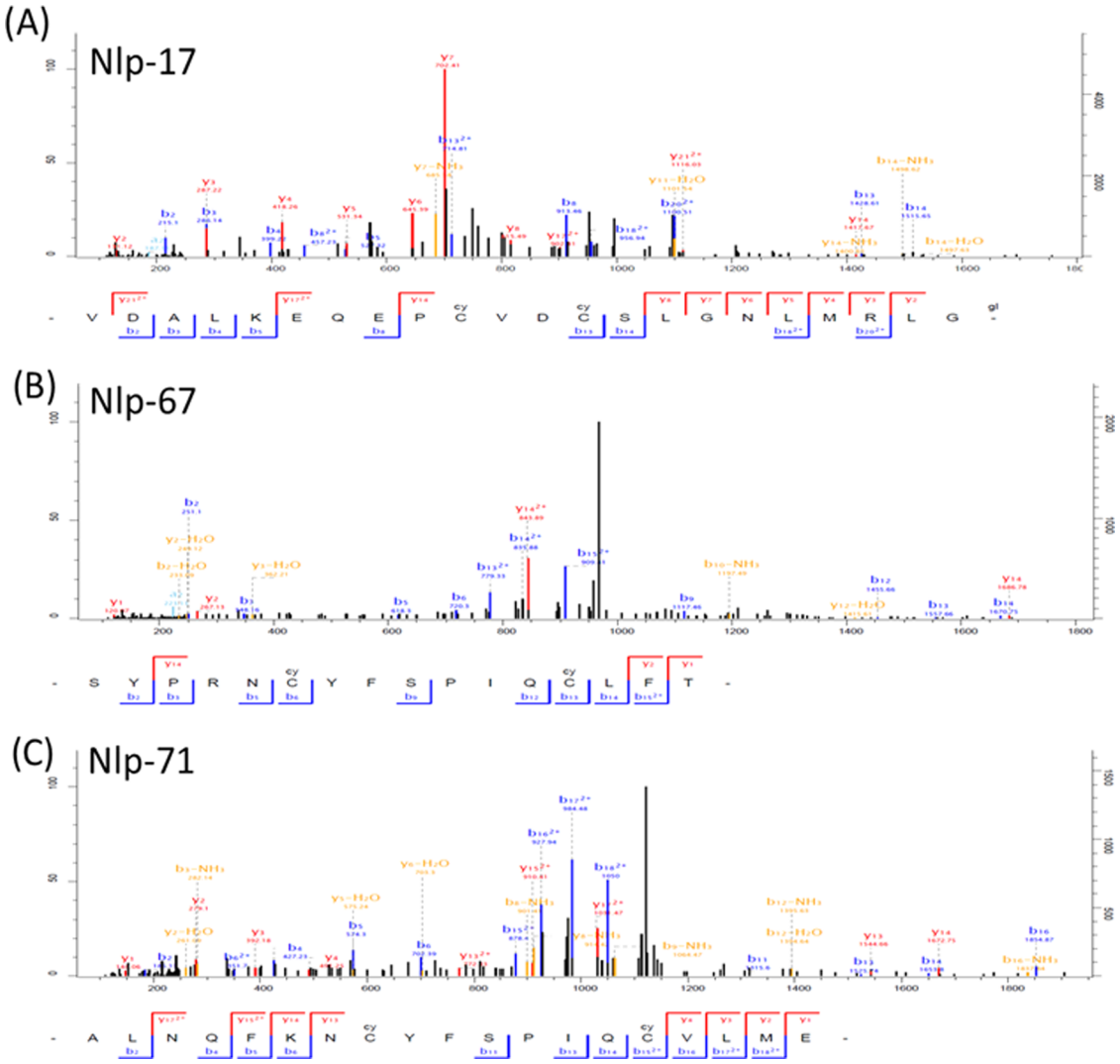

Figure 5. MS/MS spectra of the C-terminal peptides of *nlp-17* (A), *nlp-67* (B), and *nlp-71* (C) of *H. contortus*. The fragmentation schemes allow the unambiguous identification of the presence of a disulfide bridge between two cysteine residues for the three peptides.

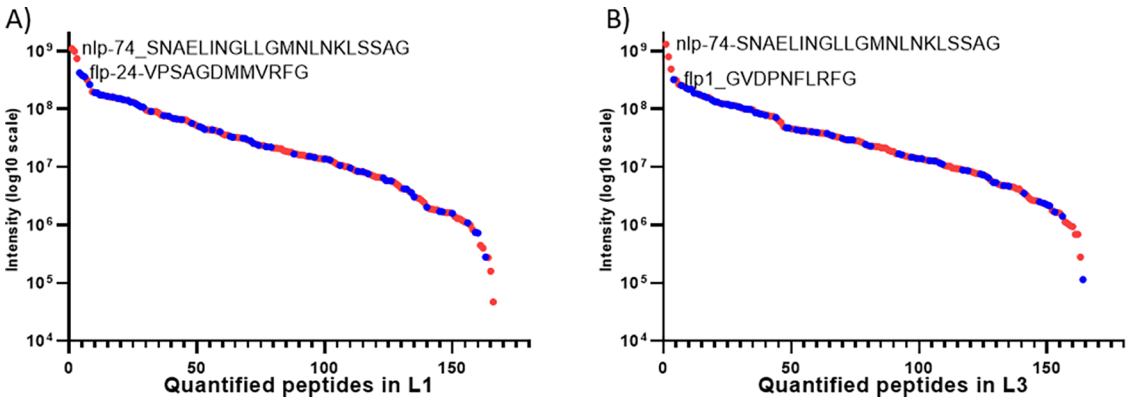

Figure 6. Relative abundance of *flp*-encoded (highlighted in blue) and *nlp*-encoded peptides (highlighted in red) in the L1 larvae stage (A) and L3 larvae stage (B) of *H. contortus*. The most intense peptides identified are indicated.

and stops actively feeding, prior to being ingested by the ruminant host. Despite these dramatic differences in life stage behaviors, which have been reflected previously through transcriptomic studies showing significant differences in protein-coding gene expression,[34,38] both life stages appear here to express mostly similar FLP and NLP neuropeptides. Among the 181 quantified peptides in this study, 170 were detected in the L1 stage and 171 in the L3 stage. This is consistent with the fact that many of these neuropeptides, especially the FLPs, regulate diverse behaviors through the modulation of sensory and motor functions.

https://doi.org/10.1021/acsomega.1c00650
ACS Omega 2021, 6, 10288−10305

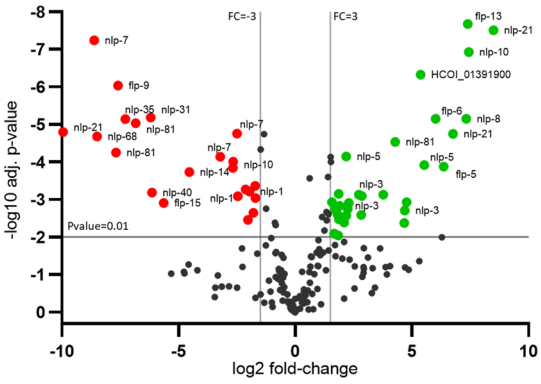

Figure 7. Volcano plot showing peptides differentially expressed between L1 larvae and L3 larvae of *H. contortus*. The *x*-axis represents the log2 fold-change (FC) of L3 versus L1. The *y*-axis represents the *p*-value from a *t* test applied between four L1 biological replicates and three L3 biological replicates. All data are shown in Table S2. Peptides with FC < −3 and *p*-value <0.01, statistically more expressed in L1 stage, are highlighted in green and peptides with FC > 3 and *p*-value <0.01, statistically more expressed in L3 stage, are highlighted in red. For the purpose of clarity, peptides are only annotated by the precursor name.

It appears that genes expressed in both life stages are overall upregulated in the L3 phase, with only peptides encoded on *flp-2*, *flp-9*, *nlp-1*, and *nlp-7* being upregulated in the L1 stages. These changes in expression could be associated with the maturation of the nervous motor system observed in L3. It is also possible that the peptides upregulated in the L1s associate with feeding behaviors that differ dramatically between the L1 and L3 life stages. More interesting is that for some genes, individual peptides are differentially expressed in one of the life stages compared to the other, e.g., *nlp-10*, *nlp-21*, *nlp-40*, and *nlp-81*. These data are intriguing and suggest that nematodes can differentially regulate the levels of individual peptides from the same precursor protein. This could be done through more rapid degradation of some component peptides compared to others, which further demonstrates the complexity inherent in nematode neuropeptide signaling.

Furthermore, the ability to quantify neuropeptides between different samples allows the comparison of peptide profiles. For example, this quantitative strategy allowed the differential analysis of peptide amidation profiles and represents an efficient approach to the characterization of key neuropeptide processing enzymes of the neuropeptide processing pathway or, in the context of drug discovery, could inform target engagement and the efficacy of inhibitors or modulators of the neuropeptide signaling pathways or their processing enzymes. This repository of biochemically identified and quantified peptide sequences provides a unique resource to enable the discovery of compounds active at different developmental stages of the nematode.

In conclusion, the extensive neuropeptide database provided here is a first step toward the understanding of the fundamental biochemistry of *H. contortus* and can be exploited in further experimental studies aiming at developing new anthelmintics against *H. contortus*.

METHODS

Parasite Collection. All *H. contortus* samples (L1 and L3 stages) were obtained from Boehringer Ingelheim Animal Health. Worms were pelleted (12 min, 1800*g*), resuspended in deionized water, and washed several times with water. At the end of the final wash, worms were resuspended in 30 μL of PBS prior to storage at −80 °C. The L1 samples had a similar biomass to the L3 stage samples, i.e., approximately 45 000 L1 and 20 000 L3 in a volume of 20 μL PBS.

Peptide Extraction and Purification. To extract the peptides, 150 μL of an acidic methanol (methanol/water/acetic acid (90/9/1)) solution was added to the larvae. The mixture was then stirred for 30 min at 4 °C, followed by a 10 s sonication step for L3 larvae. Samples were then centrifuged for 15 min at 10 000*g* at 4 °C. Supernatants were collected and concentrated under vacuum (Concentrator 5301, Eppendorf (SpeedVac)) to obtain a volume of approximately 10 μL. The peptides were purified and desalted using C18 columns (OMIX C18 pipette tips, Millipore, Molsheim, France) according to manufacturer's instructions. Finally, peptides were concentrated in vacuum and reconstituted in 0.2% formic acid for injection in LC-MS/MS.

Nano-HPLC/Nano-ESI Orbitrap-MS/MS. LC-MS/MS analyses were performed using a liquid chromatograph (LC) coupled to an Orbitrap Fusion Tribrid mass spectrometer (Thermo Fisher Scientific, San Jose, CA) using a Nano-spray Flex NG source. Reversed-phase chromatography was performed with a nano-ACQUITY Ultra-Performance LC system (Waters, Milford, MA) fitted with a trapping column (nano-Acquity Symmetry C18, 100 Å, 5 μm, 180 μm × 20 mm) at a 15 μL/min flow rate and an analytical column (nano-Acquity BEH C18, 130 Å, 1.7 μm, 75 μm × 250 mm) directly coupled to the ion source. The mobile phases for LC separation were 0.2% (v/v) formic acid in LC-MS grade water (solvent A) and 0.2% (v/v) formic acid in acetonitrile (solvent B). Peptides were separated at a 300 nL/min constant flow rate with a linear gradient of 5−85% solvent B for 85 min. A full MS1 survey scan was acquired with the Orbitrap for m/z 325−1200 at a 50 ms maximum filling time and 2×10^5 ions. The resolution was set to 120 000 at m/z 200. For MS/MS experiments, fragmentation was performed in HCD fragmentation cell (collision energy at 26%), with isolation of precursor ions in a quadrupole. Target ions previously selected for fragmentation were dynamically excluded for 50 s with a relative mass window of ±10 ppm. The MS/MS selection threshold was set to 5×10^3 ion counts. The detection was performed in an Ion Trap with an Automatic Gain Control (AGC) of 2×10^4 target value and a 50 ms maximum injection time. Each sample was injected twice (technical replicate).

Data Processing. Identification and quantification of peptides were performed using MaxQuant software (Ver. 1.5.3.8, Max-Planck Institute of Biochemistry, Department of Proteomics and Signal Transduction, Munich). Database searching was performed against the FASTA databases downloaded from the WormBase site (https://wormbase.org) (BioProject PRJNA205202 and BioProject PRJEB506). Interrogation of the databanks was based on the following criteria: precursor mass tolerance of 7 ppm, fragment ions mass tolerance of 0.6 Da, and 2 maximum missed cleavages with semi-trypsin as the enzyme. Search parameters for post-translational modifications were variable modifications of oxidation on methionine residues, N-terminal cyclization of glutamine/glutamic acid to pyroglutamate, disulfide bridge on cysteine residues, and glycine loss in combination with amidation (Gly-loss+Amide (C-term G)). The match between runs was performed with a match time window set to 0.7 min and an alignment time window set to 20 min. A false discovery

https://doi.org/10.1021/acsomega.1c00650
ACS Omega 2021, 6, 10288−10305

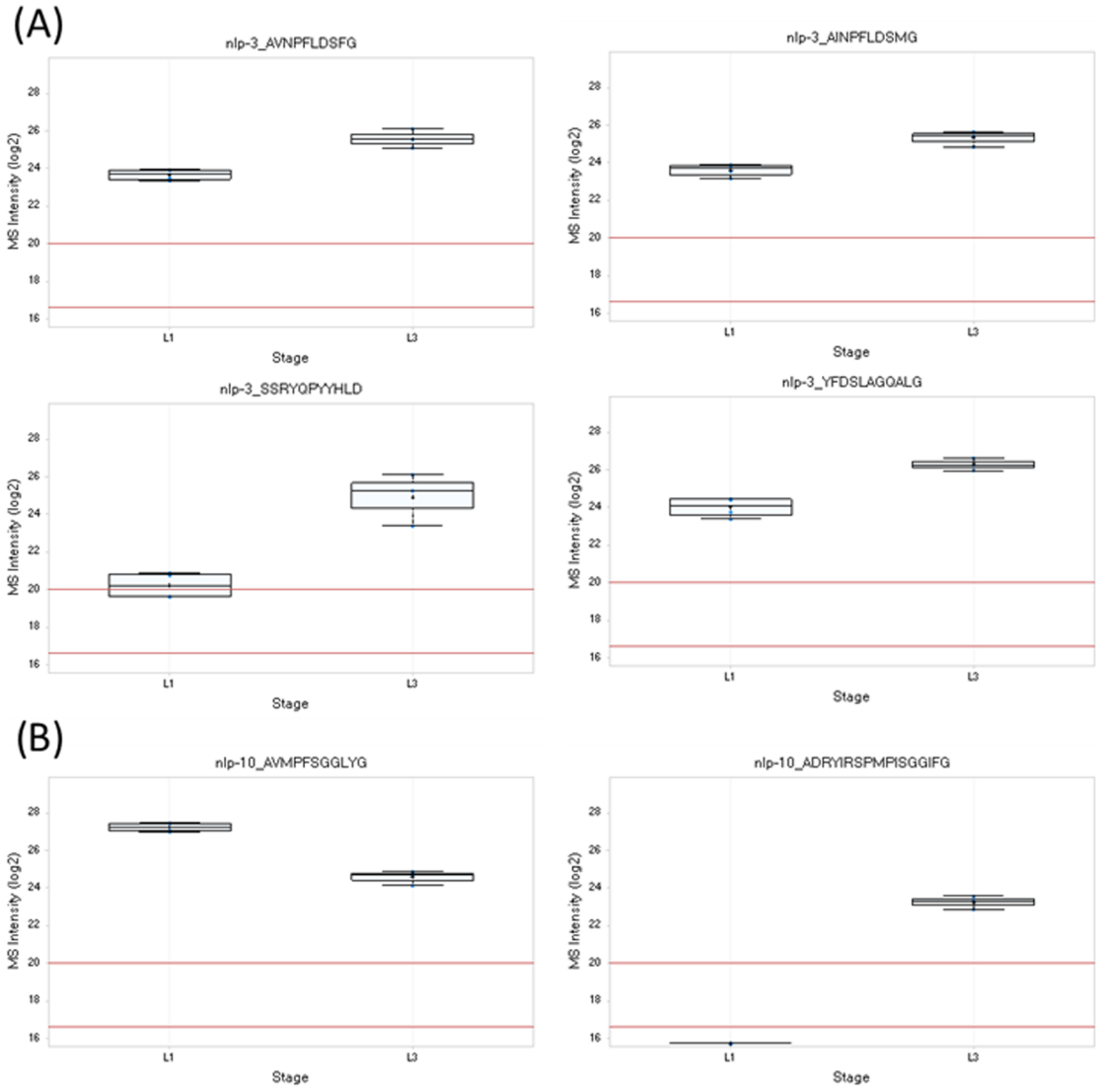

Figure 8. Relative label-free quantification of four *nlp-3* encoded peptides (A) and of two *nlp-10* encoded peptides (B) between the first-stage (L1) and third-stage larvae (L3) of *H. contortus*. The boxplots were obtained from four L1 biological replicates and from three L3 biological replicates. The zone below the inferior red line (value of 16.6) indicates very low or no expression. The zone between the two red lines corresponds to a low expression zone.

rate of 1% was required for peptides with a minimum Andromeda score for accepting an MS/MS identification for modified peptides set to 40. All of the other parameters were MaxQuant default parameters. Peptides were retained as putative neuropeptides if they were surrounded by (di)basic residues and were kept only if their Andromeda score was higher than 60 or after manual inspection of their MS/MS spectra.

Differential Statistical Analysis. Peptide intensities were exported from the MaxQuant modificationSpecificPeptides file. Missing values were replaced by the minimum value of each acquisition. Intensities were transformed into their log2 values. Medians were calculated over the technical replicates. Data normalization was performed on the set of all identified and quantified peptides. The normalization coefficients thus obtained were applied to the initial intensities of all of the peptides detected. A two-tailed *t* test for each peptide was performed on the normalized medians to determine the statistical significance between L1 and L3 sample groups, assuming equal variance.

■ ASSOCIATED CONTENT

Supporting Information

The Supporting Information is available free of charge at https://pubs.acs.org/doi/10.1021/acsomega.1c00650.

Sequence alignments of *H. contortus* FLP precursors predicted from the WormBase PRJNA205202 project and from the WormBase PRJEB506 with its homologs in *C. elegans*, UniProtKB source (Figure S1); sequence alignments of *H. contortus* NLP precursors predicted from the PRJNA205202 and from the PRJEB506.WBPS14 WormBase projects with their homologs in *C. elegans*, UniProtKB source (Figure S2); relative label-free quantification of FLP and NLP peptides between the first-stage (L1) and third-stage larvae (L3) of *H. contortus* (Figure S3); homemade database Fasta file (Supplementary Data 1) (PDF)

Blast analysis of *C. elegans* NLP precursors reported by Van Bael et al.,[29] against *H. contortus* WormBase PRJEB506 and PRJNA205202 databases (Table S1);

https://doi.org/10.1021/acsomega.1c00650
ACS Omega 2021, 6, 10288−10305

expressions of all FLP and NLP peptides in the L1 larvae stage and L3 larvae stage of *H. contortus* (Table S2); expressions of mature FLP and NLP peptides in the L1 larvae stage and L3 larvae stage of *H. contortus* (Table S3) (XLSX)

AUTHOR INFORMATION

Corresponding Author

Armelle Buzy − *Sanofi R&D, 91385 Chilly-Mazarin, France*; orcid.org/0000-0003-3084-0468; Email: armelle.buzy@sanofi.com

Authors

Camille Allain − *Sanofi R&D, 91385 Chilly-Mazarin, France*

John Harrington − *Boehringer Ingelheim Animal Health, Duluth, Georgia 30096, United States*

Dominique Lesuisse − *Sanofi R&D, 91385 Chilly-Mazarin, France*

Vincent Mikol − *Sanofi R&D, 91385 Chilly-Mazarin, France*

David F. Bruhn − *Boehringer Ingelheim Animal Health, Duluth, Georgia 30096, United States*

Aaron G. Maule − *School of Biological Sciences, Queens's University Belfast, Belfast BT9 7BL, U.K.*

Jean-Claude Guillemot − *Sanofi R&D, 91385 Chilly-Mazarin, France*

Complete contact information is available at: https://pubs.acs.org/10.1021/acsomega.1c00650

Author Contributions

A.B. wrote the paper with input from all other authors. A.B. and C.A. designed the experiments. J.-C.G. supervised the development of the whole analytical workflow. D.F.B. prepared the parasite samples for peptide extraction. C.A. performed the peptide extraction, the LC-MS/MS analysis, and the Database Searching. A.B. processed the data.

Notes

The authors declare no competing financial interest.

ACKNOWLEDGMENTS

The authors would like to thank Veeranagouda Yaligara, Michel Didier, Jean-Luc Zachayus, and Anne Remaury for technical advice.

ABBREVIATIONS

FLPs, FMRFamide-like peptides; NLPs, neuropeptide-like proteins; LC-MS/MS, liquid chromatography-tandem mass spectrometry; FDR, false discovery rate; FC, fold-change

REFERENCES

(1) Besier, R. B.; Kahn, L. P.; Sargison, N. D.; Van Wyk, J. A. The Pathophysiology, Ecology and Epidemiology of *Haemonchus contortus* Infection in Small Ruminants. *Adv. Parasitol.* **2016**, *93*, 95−143.

(2) Gasser, R. B.; von Samson-Himmelstjerna, G. *Haemonchus contortus* and haemonchosis− past, present and future trends. *Adv. Parasitol.* **2016**, *93*, 1−666.

(3) Veglia, E. The anatomy and life history of the *Haemonchus contortus*. *Rep. Dir. Vet. Res.* **1915**, *3*−*4*, 347−500.

(4) Brown, L. A.; Jones, A. K.; Buckingham, S. D.; Mee, C. J.; Sattelle, D. B. Contributions from *Caenorhabditis elegans* functional genetics to antiparasitic drug target identification and validation: nicotinic acetylcholine receptors, a case study. *Int. J. Parasitol.* **2006**, *36*, 617−624.

(5) Martin, R. J.; Robertson, A. P. Control of Nematode Parasites with Agents Acting on Neuro-Musculature Systems: Lessons for Neuropeptide Ligand Discovery. *Adv. Exp. Med. Biol.* **2010**, *692*, 138−154.

(6) Mousley, A.; Marks, N. J.; Halton, D. W.; Geary, T. G.; Thompson, D. P.; Maule, A. G. Arthropod FMRFamide-related peptides modulate muscle activity in helminths. *Int. J. Parasitol.* **2004**, *34*, 755−768.

(7) Kotze, A. C.; Prichard, R. K. Anthelmintic Resistance in *Haemonchus contortus*: History, Mechanisms and Diagnosis. *Adv. Parasitol.* **2016**, *93*, 397−428.

(8) Maule, A. G.; Mousley, A.; Marks, N. J.; Day, T. A.; Thompson, D. P.; Geary, T. G.; Halton, D. W. Neuropeptide signaling systems - potential drug targets for parasite and pest control. *Curr. Top. Med. Chem.* **2002**, *2*, 733−758.

(9) Mousley, A.; Polese, G.; Marks, N. J.; Eisthen, H. L. Terminal nerve-derived neuropeptide y modulates physiological responses in the olfactory epithelium of hungry axolotls (*Ambystoma mexicanum*). *J. Neurosci.* **2006**, *26*, 7707−7717.

(10) Mousley, A.; Novozhilova, E.; Kimber, M. J.; Day, T. A.; Maule, A. G. Neuropeptide physiology in helminths. *Adv. Exp. Med. Biol.* **2010**, *692*, 78−97.

(11) McVeigh, P.; Atkinson, L.; Marks, N. J.; Mousley, A.; Dalzell, J. J.; Sluder, A.; Hammerland, L.; Maule, A. G. Parasite neuropeptide biology: Seeding rational drug target selection? *Int. J. Parasitol.: Drugs Drug Resist.* **2012**, *2*, 76−91.

(12) McVeigh, P.; Geary, T. G.; Marks, N. J.; Maule, A. G. The FLP-side of nematodes. *Trends Parasitol.* **2006**, *22*, 385−396.

(13) Li, C.; Nelson, L. S.; Kim, K.; Nathoo, A.; Hart, A. C. Neuropeptide gene families in the nematode *Caenorhabditis elegans*. *Ann. N. Y. Acad. Sci.* **1999**, *897*, 239−252.

(14) McCoy, C. J.; Atkinson, L. E.; Zamanian, M.; McVeigh, P.; Day, T. A.; Kimber, M. J.; Marks, N. J.; Maule, A. G.; Mousley, A. New insights into the FLPergic complements of parasitic nematodes: Informing deorphanisation approaches. *EuPa Open Proteomics* **2014**, *3*, 262−272.

(15) Peymen, K.; Watteyne, J.; Frooninckx, L.; Schoofs, L.; Beets, I. The FMRFamide-Like Peptide Family in Nematodes. *Front. Endocrinol.* **2014**, *5*, 90.

(16) Gahoi, S.; Gautam, B. Identification and analysis of insulin like peptides in nematode secretomes provide targets for parasite control. *Bioinformation* **2016**, *12*, 412−415.

(17) Price, D. A.; Greenberg, M. J. Structure of a molluscan cardioexcitatory neuropeptide. *Science* **1977**, *197*, 670−671.

(18) McVeigh, P.; Alexander-Bowman, S.; Veal, E.; Mousley, A.; Marks, N. J.; Maule, A. G. Neuropeptide-like protein diversity in phylum Nematoda. *Int. J. Parasitol.* **2008**, *38*, 1493−1503.

(19) Nathoo, A. N.; Moeller, R. A.; Westlund, B. A.; Hart, A. C. Identification of neuropeptide-like protein gene families in *Caenorhabditis elegans* and other species. *Proc. Natl. Acad. Sci. U.S.A.* **2001**, *98*, 14000−14005.

(20) Li, C.; Kim, K. Family of FLP Peptides in *Caenorhabditis elegans* and Related Nematodes. *Front. Endocrinol.* **2014**, *5*, 150.

(21) Christie, A. E.; Nolan, D. H.; Garcia, Z. A.; McCoole, M. D.; Harmon, S. M.; Congdon-Jones, B.; Ohno, P.; Hartline, N.; Congdon, C. B.; Baer, K. N.; Lenz, P. H. Bioinformatic prediction of arthropod/nematode-like peptides in non-arthropod, non-nematode members of the Ecdysozoa. *Gen. Comp. Endocrinol.* **2011**, *170*, 480−486.

(22) Jarecki, J. L.; Frey, B. L.; Smith, L. M.; Stretton, A. O. Discovery of neuropeptides in the nematode *Ascaris suum* by database mining and tandem mass spectrometry. *J. Proteome Res.* **2011**, *10*, 3098−3106.

(23) Koziol, U.; Koziol, M.; Preza, M.; Costabile, A.; Brehm, K.; Castillo, E. De novo discovery of neuropeptides in the genomes of parasitic flatworms using a novel comparative approach. *Int. J. Parasitol.* **2016**, *46*, 709−721.

(24) McCoy, C. J.; Atkinson, L. E.; Robb, E.; Marks, N. J.; Maule, A. G.; Mousley, A. Tool-Driven Advances in Neuropeptide Research

from a Nematode Parasite Perspective. *Trends Parasitol.* **2017**, *33*, 986−1002.
(25) Edwards, S. L.; Mergan, L.; Parmar, B.; Cockx, B.; De Haes, W.; Temmerman, L.; Schoofs, L. Exploring neuropeptide signalling through proteomics and peptidomics. *Expert Rev. Proteomics* **2019**, *16*, 131−137.
(26) Husson, S. J.; Clynen, E.; Baggerman, G.; De Loof, A.; Schoofs, L. Discovering neuropeptides in *Caenorhabditis elegans* by two dimensional liquid chromatography and mass spectrometry. *Biochem. Biophys. Res. Commun.* **2005**, *335*, 76−86.
(27) Husson, S. J.; Landuyt, B.; Nys, T.; Baggerman, G.; Boonen, K.; Clynen, E.; Lindemans, M.; Janssen, T.; Schoofs, L. Comparative peptidomics of *Caenorhabditis elegans* versus *C. briggsae* by LC-MALDI-TOF MS. *Peptides* **2009**, *30*, 449−457.
(28) Van Bael, S.; Edwards, S. L.; Husson, S. J.; Temmerman, L. Identification of Endogenous Neuropeptides in the Nematode *C. elegans* Using Mass Spectrometry. *Methods Mol. Biol.* **2018**, *1719*, 271−291.
(29) Van Bael, S.; Zels, S.; Boonen, K.; Beets, I.; Schoofs, L.; Temmerman, L. A *Caenorhabditis elegans* Mass Spectrometric Resource for Neuropeptidomics. *J. Am. Soc. Mass Spectrom.* **2018**, *29*, 879−889.
(30) Yew, J. Y.; Dikler, S.; Stretton, A. O. De novo sequencing of novel neuropeptides directly from *Ascaris suum* tissue using matrix-assisted laser desorption/ionization time-of-flight/time-of-flight. *Rapid Commun. Mass Spectrom.* **2003**, *17*, 2693−2698.
(31) Keating, C. D.; Holden-Dye, L.; Thorndyke, M. C.; Williams, R. G.; Mallett, A.; Walker, R. J. The FMRFamide-like neuropeptide AF2 is present in the parasitic nematode *Haemonchus contortus*. *Parasitology* **1995**, *111*, 515−521.
(32) Marks, N. J.; Sangster, N. C.; Maule, A. G.; Halton, D. W.; Thompson, D. P.; Geary, T. G.; Shaw, C. Structural characterisation and pharmacology of KHEYLRFamide (AF2) and KSAYMRFamide (PF3/AF8) from *Haemonchus contortus*. *Mol. Biochem. Parasitol.* **1999**, *100*, 185−194.
(33) Laing, R.; Kikuchi, T.; Martinelli, A.; Tsai, I. J.; Beech, R. N.; Redman, E.; Holroyd, N.; Bartley, D. J.; Beasley, H.; Britton, C.; Curran, D.; Devaney, E.; Gilabert, A.; Hunt, M.; Jackson, F.; Johnston, S. L.; Kryukov, I.; Li, K.; Morrison, A. A.; Reid, A. J.; Sargison, N.; Saunders, G. I.; Wasmuth, J. D.; Wolstenholme, A.; Berriman, M.; Gilleard, J. S.; Cotton, J. A. The genome and transcriptome of *Haemonchus contortus*, a key model parasite for drug and vaccine discovery. *Genome Biol.* **2013**, *14*, R88.
(34) Schwarz, E. M.; Korhonen, P. K.; Campbell, B. E.; Young, N. D.; Jex, A. R.; Jabbar, A.; Hall, R. S.; Mondal, A.; Howe, A. C.; Pell, J.; Hofmann, A.; Boag, P. R.; Zhu, X. Q.; Gregory, T.; Loukas, A.; Williams, B. A.; Antoshechkin, I.; Brown, C.; Sternberg, P. W.; Gasser, R. B. The genome and developmental transcriptome of the strongylid nematode *Haemonchus contortus*. *Genome Biol.* **2013**, *14*, R89.
(35) Atkinson, L. E.; Miskelly, I. R.; Moffett, C. L.; McCoy, C. J.; Maule, A. G.; Marks, N. J.; Mousley, A. Unraveling flp-11/flp-32 dichotomy in nematodes. *Int. J. Parasitol.* **2016**, *46*, 723−736.
(36) Li, C.; Kim, K.; Nelson, L. S. FMRFamide-related neuropeptide gene family in *Caenorhabditis elegans*. *Brain Res.* **1999**, *848*, 26−34.
(37) Petrushin, A.; Ferrara, L.; Blau, A. The Si elegans project at the interface of experimental and computational *Caenorhabditis elegans* neurobiology and behavior. *J. Neural Eng.* **2016**, *13*, No. 065001.
(38) Ma, G.; Wang, T.; Korhonen, P. K.; Ang, C. S.; Williamson, N. A.; Young, N. D.; Stroehlein, A. J.; Hall, R. S.; Koehler, A. V.; Hofmann, A.; Gasser, R. B. Molecular alterations during larval development of *Haemonchus contortus* in vitro are under tight post-transcriptional control. *Int. J. Parasitol.* **2018**, *48*, 763−772.

https://doi.org/10.1021/acsomega.1c00650
ACS Omega 2021, 6, 10288−10305